345

ALTERNATING CURRENT (AC) RESISTANCE OF HELICALLY STRANDED CONDUCTORS

Working Group
B2.12

April 2008

April 2008

Alternating current (ac) resistance of helically stranded conductors

WG B2.12

Members of the WG:

D. Douglass (USA) ; M. Gaudry (FR) ; T. Seppa (USA) ; R. Stephen (ZA)
D. Muftic (ZA) ; S. Ueda (BR); A. Goel (CA) ; R. Kimata (JP)
S. Hoffman (UK) ; J. Iglesias-Diaz (ES) ; F.Massaro (IT
B. Risse (BE) ; L. Varga (HU) ; V.T. Morgan (AU)

ISBN: 978- 2- 85873- 033- 9

Table of contents

SUMMARY

The electrical resistance of helically-stranded conductors (aluminium and aluminium alloy), intended for use in distribution and transmission lines, depends on the conductor cross-section area, the conductivity of the aluminium alloy, the lay length of the aluminium layers, and the presence or absence of a steel reinforcing core. The presence of a stranded steel core both reduces the conductor resistance due to the conductivity of the galvanized steel wires and increases the resistance due to core magnetizing effects. This brochure describes a process of calculation for stranded aluminium conductors both with and without a steel reinforcing core.

APPENDIX A provides a MathCad programme to determine the AC resistance of a stranded conductor for a given current. This output can be used in conjunction with the steady state model to determine the actual current flow or conductor temperature.

Note that the programme shown in Appendix A follows exactly the work done by Barret et al. Care should be taken, however, when using this programme to determine the exact AC resistance of ACSR conductors in order, for example to replicate present AC resistance curves supplied by manufacturers. The differences in measuring techniques (length of sample used), the lay lengths, magnetic properties of the core, and other factors may give different results. The programme is thus suitable for determining the effect of these parameters on AC resistance and comparing different conductor designs.

APPENDIX B provides an alternate model for the calculation of the AC resistance

On the basis of laboratory tests and theoretical studies, it has been determined, that AC resistance of stranded aluminium conductors (AAC) or all aluminium conductors (AAAC) can be calculated with acceptable accuracy by taking into consideration the conductor geometry, e.g. lay ratio, diameter of wire, current and temperature distribution of conductor. Resistance calculations with Aluminium conductor Steel reinforced (ACSR), however, can be more complex due interactions between the currents in each helically stranded layer coupled through the steel core.

On the basis of results from research [5,6,7,8]* computer programs have been developed that can determine the AC resistance of ACSR very accurately (one presented here). This brochure describes the theory as well as demonstrating a programme that can be used within existing software packages that will enable rapid and accurate determination of AC resistance for helically stranded conductor types.

Layout of the document

The document covers the historical research into AC resistance and covers the different factors that make up the AC resistance of conductors. One of the main effects that has only been taken into account in recent times is the different current densities in each layer of the conductor. The programmes shown in the appendices (flowchart and Math Cad code) are based on different methods to determine the different currents in each layer.

In order to determine the AC resistance of an ACSR conductor you need to take into account the following:-

DC resistance –	depends on the resistivity and length of the strand.
Temperature –	increased temperature increases the DC resistance
Skin effect –	this increases the current in the outer section of the strand and also tends to force the current to the outer layers of the conductor.
Core losses –	this is due to eddy current and magnetic hysteresis induced in the steel core and increases the temperature of the conductor hence the Direct Current (DC) resistance component.
Transformer effect –	This effect produces induced currents in the wires as a result of magnetization of the steel core. thereby increasing the current density in the middle layer of a three layer aluminium conductor. This is described in detail in [44] and [45].

The methods described can determine the AC resistance for all types of conductors. In homogeneous conductors, the skin and temperature effects are most important.

* The research is sponsored by Fund of the National Science and Research (OTKA) T 014 372, T 016 078

1 INTRODUCTION

Bare stranded aluminium conductors, with and without steel reinforced cores, have been used for over 80 years for the transmission of electric power at high voltage. These conductors consist of one or more layers of aluminium wires stranded concentrically (with alternate right-hand and left-hand directions). When steel reinforced, the conductor core consists of one or more galvanized steel wires. The steel core and aluminium layers provide mechanical strength, but the aluminium wires carry most of the current.

Whether there is a steel core or not, alternating current flowing in the aluminium wires causes skin effect within the conductor and, at frequencies of 50 to 60 Hertz, skin effect increases the resistance by between 1% and 10% for conductors having diameters of from 20 to 50 mm, respectively..

In ACSR, the alternating current produces an alternating axial magnetic flux in the steel core which further changes the current distribution between aluminium layers, and increases the effective ac resistance by as much as 5% to 20% for three-layer and single layer ACSR.
.
The accuracy of any resistance calculation for bare aluminium stranded conductor is complicated by the following factors:

- Electrical contact can be made only with the outer layer of wires, unless compression fittings are used.
- The electrical contacts between wires in the same layer and wires in adjacent layers may depend on the degree of oxidation and the tension in the conductor.

The conductor is not isothermal, since there will be a radial temperature gradient, and there may also be a longitudinal temperature gradient.

2 DIRECT CURRENT PARAMETERS

With direct current, the current density within an isothermal solid cylindrical or tubular conductor is uniform. Provided that good contact is made with all the strands, the distribution of the current density within an isothermal homogeneous stranded conductor carrying direct current is also uniform. In the case of a bimetallic conductor, such as ACSR, the current density within each metallic section is inversely proportional to the resistivity of that section.

2.1 Calculation of DC resistance for bare stranded aluminium conductors

The resistance per unit length R of a conductor depends on the resistivity ρ and the cross-sectional area A. Since the resistivity is temperature dependent, the resistance also varies with the temperature T of the conductor.

The DC resistance per unit length of a solid cylindrical conductor is calculated from:

$$R_{dc} = 4\,\rho_{20}\,[1 + \alpha_{20}\,(T - 20)] / \pi\,D_s^2 \qquad (1)$$

where ρ_{20} and α_{20} are the resistivity and its temperature coefficient, respectively, at 20 °C , T is the temperature of the conductor and D_s is the outer diameter of the conductor.:

Stranding of a conductor increases its length. The resistance per unit length of a stranded homogeneous conductor is calculated from:

$$\frac{1}{R_{dc}} = \frac{\pi d^2}{4\rho}\left(1 + \sum_1^n \frac{6n}{k_n}\right) \qquad (2)$$

where d is the diameter of each wire, n is the number of the layers, and k_n is a length factor, found calculated as follows:

$$k_n = \left[1 + \left(\frac{\pi D_n}{\lambda_n}\right)^2\right]^{1/2} \qquad (3)$$

where D_n is the mean diameter of layer n and λ_n is the lay length of that layer. The ratio λ_n/D_n is known as the lay ratio of layer n. In the case of a stranded bimetallic conductor, such as ACSR, the DC resistance can be calculated from:

$$\frac{1}{R_{dc}} = \frac{\pi d_s^{\,2}}{4\rho_s}\left(1 + \sum_1^{n_s} \frac{6n_s}{k_{ns}}\right) + \frac{\pi d_a^{\,2}}{4\rho_a}\left(1 + \sum_{n_a+1}^{n_a} \frac{6n_a}{k_{na}}\right) \qquad (4)$$

where the subscripts a and s refer to the nonferrous and ferrous sections, respectively.

3 ALTERNATING CURRENT PARAMETERS

In order to determine the parameters that affect AC resistance, it is necessary to study the effects on the resistive and the internal inductance.

3.1 Parameters that affect AC resistance

3.1.1 Effect of current

The current density distribution within any conductor carrying alternating current is rarely uniform. With solid cylindrical and tubular homogeneous conductors, there are skin and proximity effects. With stranded homogeneous conductors, variable contact resistances between strands may also affect the current distribution. With stranded steel-cored aluminium conductors (ACSR) the alternating magnetic flux in the core may cause hysteresis and eddy current losses in the core and a profound redistribution of current density in the layers of non-ferrous wires [8,11,14,15,16].

3.1.2 Effect of frequency (skin effect)

The AC resistance of any conductor depends on the frequency of the current, as this determines the magnitude of the skin effect. At power frequency, there is usually negligible variation in the resistance with frequency in the case of a monometallic conductor. With steel-cored conductors, such as ACSR, however, there may be a significant effect of frequency, because the radial distribution of current density in the nonferrous section and the power loss in the steel core both depend on the frequency [36, 37].

Since not all the magnetic flux due to filaments of alternating current near the centre of a homogeneous conductor cuts the whole conductor, the inductance per unit area will decrease towards the surface. Hence, the current per unit area will increase towards the surface of the conductor. Theoretical studies give factors [17,18] for skin effect calculation, that is the ratio between the AC and DC resistances, for an isolated non-magnetic solid circular cylinder with negligible capacitive current as a function of conductor radius.

Theoretical studies based on measured results have proposed an explicit solution to equation for power frequencies, where the error varies from 1.6 % to 3.8 % [19]. In the case of a stranded non-magnetic conductor this includes the skin effect factor, provided that the DC resistance is calculated at the temperature of interest [20]. For steel-cored conductors, such as ACSR, some authors [21] have used for calculation the diameter of the steel core, but this neglects the effect of the magnetic flux in the core on the skin effect.

If the current density in each layer is assumed to be uniform, the outer and inner magnetic fluxes associated with each layer are given by:

$$\Phi_{n,\,outer} = (1/2\pi)\,(I_s + I_1 + \ldots k_1 I_n)\,\mu_0 \ln [D_n / (D_n - d)]$$

and

$$\Phi_{n,inner} = (1/2\pi)\,(I_s + I_1 + \ldots k_2 I_n)\,\mu_0 \ln [(D_n - d) / D_{n-1}] \qquad (5)$$

where the coefficients k_1 and k_2 take account of the fact that the layer currents are not concentrated at the centre of each layer [5]. According to theoretical study [14] calculated values for Grackle ACSR conductors are given as $k_1 = 0.79$ and $k_2 = 0{,}21$. However, according to other study[35], the calculated values for Grackle were $k_1 = 0.74$ and $k2 = 0.26$. The mutual inductive reactances due to the circular flux can be calculated from:

$$X_{n,outer} = j\,f\,\mu_0\,\Phi_{n,outer}$$

and

$$X_{n,inner} = j\,f\,\mu_0\,\Phi_{n,inner} \qquad (6)$$

Note that in discussions with Barret in March 2006, it was discovered that shortly after publishing the paper [14], that a FORTRAN program CONRES was written to compute ac resistance of ACSR with any number of layers, both standard roud wire nad trap wire. At that time some minor changes and corrections were made:-

- For round wires: k_1 and k_2 were corrected to 0.71 and 0.29 (previously 0.79 and 0.21 in [14]).

- For trapezoidal wires k_1 and k_2 were corrected to 0.67 and 0.33 (previously 0.75 and 0.25 in [14])

Note that these changes are minor and result in an ac resistance change of less than 0.1 percent.

3.1.3 Proximity effect

When two conductors carrying opposite, alternating current are parallel and close together the current densities on the sides facing each other are increased, and those on the remote sides are decreased, due to non-uniform magnetic inductions [21,22,23] . If the two currents are in the same direction, the reverse is true. In overhead power lines, bare conductors are rarely close enough for the proximity effect to be significant. This is not true, of course, for insulated power cables which can be much closer together.

3.1.4 Effect of temperature

Temperature has a significant effect on the resistance of most aluminium (and copper) conductors. The increase in dc resistance with temperature amounts to approximately 4% for every 10 degrees C change in conductor temperature. At extremely high operating current densities, the core temperature may be significantly higher than that of the outer aluminium layer and this radial temperature difference should be considered in calculating high temperature sags, particularly with ACSR where all the tension is in the core at high temperatures.

3.1.5 Iron losses excluding transformer effect.

The following equation was used prior to the inclusion of the transformer effect [24] to calculate the increase of resistance ΔR due to iron losses in the steel core. It was assumed that the current density in the non-ferrous section was uniform, and that the layer currents followed the spiralling wires, with no axial leakage because of the surface oxide layers:

$$\Delta R = 2\pi f \mu_r \mu_0 A_s N \tan\delta \tag{7}$$

$$N = \frac{\sum_{i=1}^{j} \frac{n_i}{\lambda_i}(-1)^i}{n} \tag{8}$$

where N = effective number of turns per unit length
A_s = cross-sectional area of steel core
n_i = number of wires in layer i
n = total number of non-ferrous wires
j = number of layer of non-ferrous wires.
f = frequency
μ_r = relative permeability of core
μ_0 = permeability of free space
λ_i = lay length of layer i
δ = phase angle between total current and voltage induced in non-ferrous wires

The phase angle change depends on loading current of conductor as presented in the studies [5,6,7,8]. The core losses have usually been measured [5,25,26,27,28,29].

3.1.6 Transformer effect

.

Earlier analyses [30, 31] modelled the effect of the steel core in an ACSR conductor by employing equivalent circuits, but these models identified the core loss with each layer of the conductor, rather than with the core, although they did indicate non-uniform distribution of current density between the layers of aluminium wires. The first model [32] to include the layer resistances and inductances due to the circular and longitudinal magnetic fluxes employed complex values for the layer currents, but not for the permeability of the core and the magnetic loss angles These discrepancies were partially rectified in [33], and fully accounted for in [14]. The effects of the temperature and the tensile stress in the conductor on the permeability of the core were analysed in [34].

The complex self-inductive reactances of the layers of aluminium wires, due to the longitudinal magnetic flux in the core, are calculated from:

$$X_{nn} = 2 \pi f \mu_0 \{ [(\pi / 4) D_n^2 - A_s] + \mu_r A_s\} / \lambda_n^2 \qquad (9)$$

where f is the frequency,

D_n is the mean diameter of layer n

λ_n is the lay length of layer n,

A_s is the cross-sectional area of the steel core

μ_r is the complex relative permeability of the core, and

μ_0 is the permeability of free space.

The complex mutual inductive reactances due to the longitudinal magnetic flux are calculated from:

$$X_{pq} = 2 \pi f \mu_0 \{ [(\pi / 4) D_p^2 - A_s] + \mu_r A_s\} / \lambda_p \lambda_q$$

and

$$X_{qp} = X_{pq} \qquad (10)$$

where D_p is the mean diameter of layer p, and λ_p and λ_q are the lay lengths of layers p and q, respectively.

It was shown both analytically and experimentally in [14] that both the current density and its phase angle vary both within and between layers. To study these distributions in greater detail [8,15,34] it was assumed that each wire was cut into ten annular slices, with their boundaries consisting of circular arcs having their centres at the centre of the conductor. This enabled the skin effect in each layer to be determined. It was also shown that both the current density and the phase angle in the middle layer of an ACSR conductor having three layers of aluminium wires are enhanced at the expense of the inner and outer layers. This is in agreement with other calculations [6, 16, 21] and measurements [8, 21].

3.2 Parameters that affect AC conductor impedance (Z)

The nonuniform distribution of the current density in a conductor, due to the skin effect and the transformer effect, also influences the internal inductance, particularly with steel-cored conductors, such as ACSR. In early research work the total inductance of parallel conductors was measured, but the mutual inductance usually is much larger than the internal inductance. The internal inductance can be measured with complex compensator [5,7,36]

3.2.1 Effect of current

The measurements [5,7,36,39] show that the internal inductance of an ACSR increases sinuosoidally with increasing current to a maximum value, at which magnetic saturation of the steel sets in, and then decreases as the current increases further. Fig.1. shows the variation of internal inductance with respect to loading current of ACSR conductor.

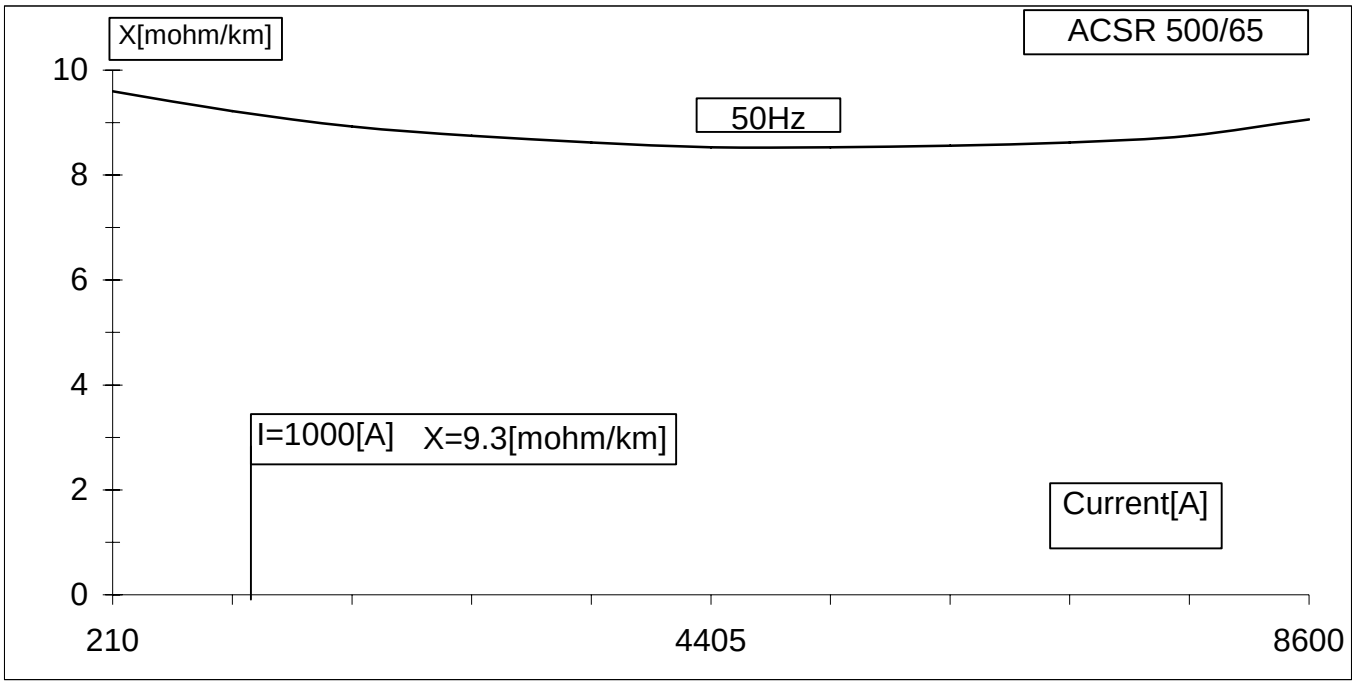

Fig. 1.

Variation of internal inductance with respect to loading current (ACSR 500/65)

3.2.2 Effect of frequency

Based on measurements and theoretical studies to the variation of internal inductance with respect to frequency can be calculated[37]. The internal inductance of an ACSR conductor decreases as the frequency increases (in the range 25 Hz to 60 Hz). The electromagnetic model [6,8,14] can be used to calculate the variation of the internal inductance of ACSR conductors. The calculated and measured results show that the inductance decreases uniformly as the frequency increases.

3.2.3 Effect of temperature

It is difficult to study the effect of temperature on the internal inductance of a conductor carrying an alternating current, because the temperature increases, even if the current is kept constant [37]. With incease temperature of aluminium layers, the current distribution of aluminium part of conductors, and eddy current in steel core also change[5,7,39]. The effect of temperature variation can be calculated using of the transformer model [5,6,7,8].

3.2.4 Effect of tensile stress

Increasing tensile stress appears to have a negligible effect on the resistance of a stranded monometallic conductor, but, in the case of a stranded steel-cored conductor, such as **ACSR**, the modulus of the relative permeability at constant magnetic field strength decreases with increasing tensile stress in the range 0 – 290 MPa [28], hence the AC resistance decreases slightly with increasing tensile stress. This is due to the Villari effect with positive magnetostriction, and is in qualitative agreement with the results for single galvanized steel wires [28]. There is a small increase in relative permeability between zero stress and about 50 MPa, due to plastic strain of the steel.

3.3 AC/DC Resistance Ratio

A general solution for the ratio of the ac resistance to the dc resistance (the "AC/DC resistance ratio") of an isolated solid non-magnetic conductor having circular cross-section has been given [18, 32]. General solutions for the resistance ratio of an isolated non-magnetic tubular conductor [20, 32] and two equal parallel non-magnetic conductors forming a single-phase system [2, 35] have also been given. The resistance of a conductor carrying an alternating current is greater than when the conductor carries a direct current of the same magnitude at the same temperature. In the case of a monometallic solid or stranded conductor, the increase in resistance is due to skin effect and, possibly, proximity effect.

In the case of ACSR, the presence of the steel core gives rise to magnetic hysteresis, eddy currents and the redistribution of current density between the layers of nonferrous wires [36]. The magnetic core loss due to hysteresis and eddy currents causes part of the voltage drop across the longitudinal reactance element in each layer to become in phase with the current in that layer. Hence the resistance of that layer is increased.

In addition to the increase in the resistance of each nonferrous layer, the distribution of the current between the layers of nonferrous wires differs from the distribution with direct current or with alternating current, with skin effect alone. It has been shown, both experimentally and analytically [6,8,14,15,16], that the current density and its phase in the middle aluminium layer of a three-layer ACSR conductor are greater than those in the inner and outer layers. The wires in each layer also exhibit skin effect, the magnitude depending on the position of the layer [6,8,15, 33, 36]. The final distribution of current may be taken as that distribution which is brought about by the transformer effect to result in the minimum total power loss in the conductor [5,6,7,8,11,13,15, 33, 36].

Higher resistance ratios occur with ACSR conductors having an odd number of layers of aluminium wires, because the cancellation of the magnetic flux in the steel core, caused by the currents spiralling in opposite directions in adjacent layers is incomplete. The highest resistance ratios occur with ACSR conductors having a single layer of aluminium wires, and

the lowest ratios occur with two-layer conductors. In order to reduce the resistance ratio with three-layer conductors, the lay lengths of the individual layers have been manipulated. However, some combinations of lay lengths are impractical to manufacture [5,6,7,8,11].

4 DETERMINATION OF EFFECT OF UNEVEN CURRENT DISTRIBUTION ON AC RESISTANCE OF ACSR CONDUCTORS.

The permissible loading current is determined by the maximum permissible temperature for the material of the conductor, the heat absorption depending on the meteorological parameters and by the heat output. Loading current value is determined on the basis of permissible temperatures of aluminium part of standing conductors, which are determined by metallurgical tests displaying no reduction of mechanical tensile strength during the expected service life of the overhead line.

Methods widely used for calculation of the current load of stranded conductors according to the literature consider the conductor to be a homogeneous heat source from a thermal point of view. In these methods, the formula of thermal equilibrium applicable to a homogeneous heat source is written for the surface [5,6,7,8,41,42, 43, 44] and the current density of conductor is assumed to be constant. Methods widely used for calculation of Joule-loss of conductors use the DC resistance of conductors, which can be found in standards, and manufacturer literature. It was found that in case of conductors of a large cross section and conductor with steel core, the difference are about 10 % between calculated and measured values of conductor temperature. According to test results, for the determination of Joule-loss, it is useful to use the AC resistance taking into consideration the temperature and current distribution within stranded conductors with steel core [45, 46].

4.1 Conventional calculating method with homogeneous current distribution

During the research mostly the Morgan's method (published in 1965 [44]) was used for the calculation of the loss of the multilayer ACSR conductors. Morgan assumed equal current-distribution in the aluminum (AL) layers for the calculation of the axial magnetic field, therefore only the iron loss was taken into in the calculation of the AC. resistance. In 1959. Match and Lewis determined that the iron loss depended on the magnetic field strength and introduced a method of measurement of the iron loss [47].
For calculation of the axial magnetic field strength taking place in the interior of a stranded conductor with more aluminium layers, the aluminium layers were replaced by one single coil with a number of turns per meter according to the following formula:

$$N = \frac{\sum_{i=1}^{j} \frac{n_i}{h_i}(-1)^i}{n} \quad (turns/m) \qquad (11)$$

where

N : number of turns per meter in the coil (turns/m),
ni : number of aluminium wires in layer i
hi : pitch of aluminium wires in layer i (m),

n : number of aluminium wires of conductors
j : number of conductor layers

Using relationship (1), increase in resistance was calculated as follows

$$\Delta R = \frac{\mu A_v \left(\sum_{i=1}^{j} \frac{n_i}{h_i} (-1)^i \right)^2 \omega}{n^2} \cdot tg\Phi \quad (\Omega / m) \tag{12}$$

where
μ : permeability of the steel core in case of a field strength (Vs/Am)
Φ : phase angle between loading current and voltage induced in the aluminium layer(°)
ω : angular frequency (rad/s)
Av : steel core cross section (m^2)
Although Morgan's calculated and measured results seemed to fit each other, neither the homogeneous current distribution among the Al layers, nor the homogenate of the magnetic field in the steel core was proved.

4.2 Laboratory testing and detection of uneven current distribution of ACSR conductors

The laboratory tests conducted to measure the current distribution among the aluminium layers by measuring the temperature rise of the aluminium layers and steel core under short-circuit conditions with the thermocouples built in between the wires (Fig. 2.) [5,6, 7, 8], depicted uneven current distribution.

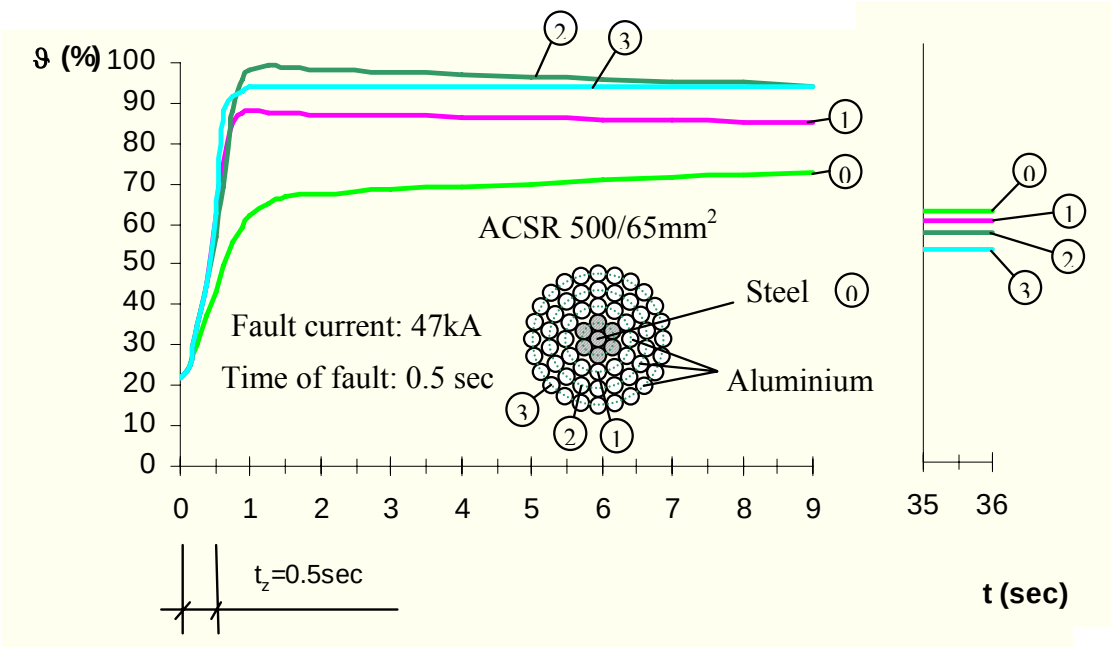

Fig. 2.
Temperature rise in ACSR conductor under short-circuit

Highest current intensity could be detected in the middle layer. The temperature distribution in conductor depends on uneven current distribution of aluminium layers. Increase of

resistance of ACSR conductor depends on value of axial exciting flux, which causes the uneven current distribution of aluminium layers. The uneven current distribution was detected also by short-circuit test (Fig 3.) [48]. The test results of VEIKI were confirmed by F. Jakl, who carried out short-circuit tests on ACSR conductor[49].
The uneven current distribution of three layers in ACSR conductor results in the AC resistance being about 5-8 % higher than DC resistance. The uneven current distribution was detected under steady-state conditions by coils built in between aluminium layers too (Fig. 4.and Fig.5.) [7,8]. The turns of coils were parallel with axes of conductors, so the induced voltage in the coil is proportional to the current of conductor layers flowing within the coil. The axial flux of steel core can be characterised by deviation of current density of the layers from homogeneous current density.
The uneven current distribution was also proven by Barrett and Findlay with measurements and calculation [45,46].

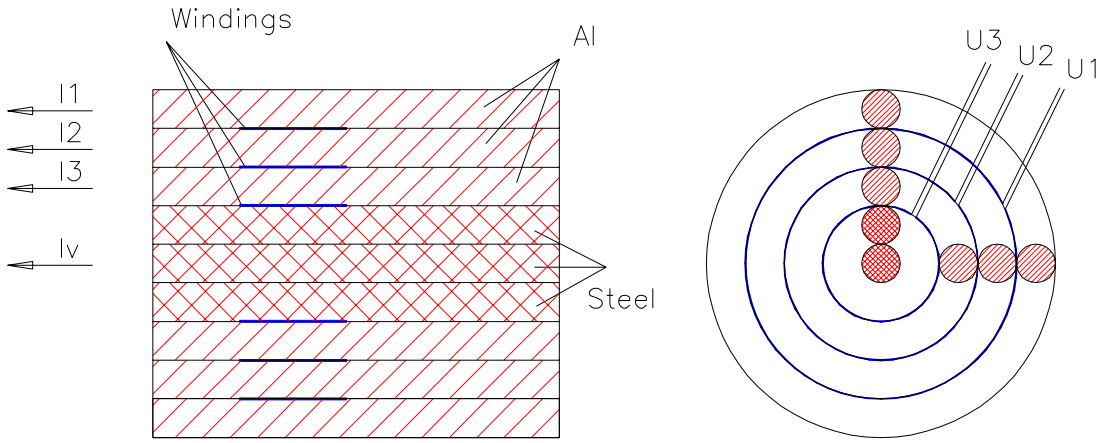

Fig. 3.
Measurement setup of current distribution measuring

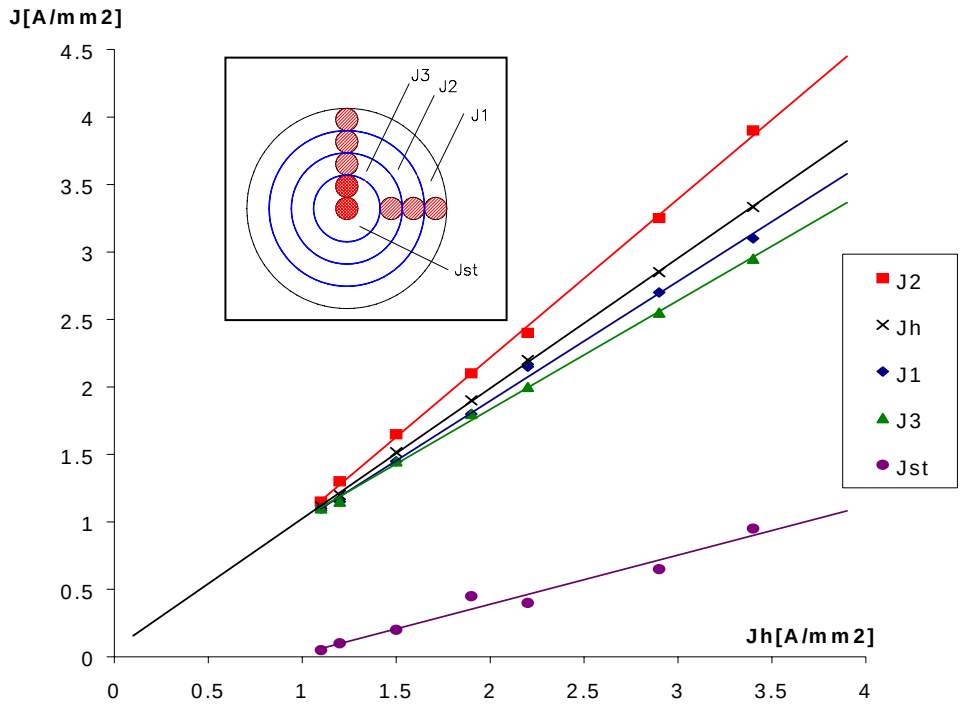

Fig. 4.
Measuring results of current distribution

Fig.4. shows current density of aluminium layers as a function of homogenous current density of the three aluminium layers.

4.3 Theoretical explanation for the uneven current distribution in the aluminum (Al) layers of ACSR conductors

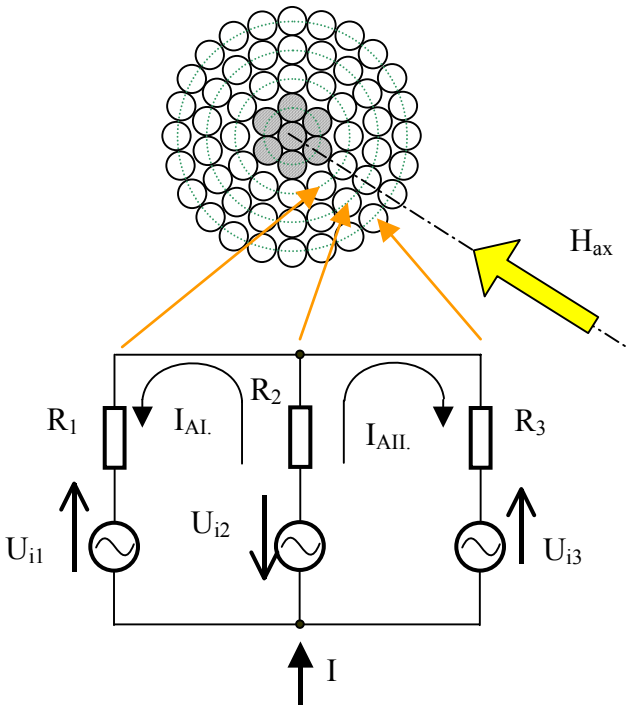

Fig. 5.
Induced voltages and currents in aluminium layers of a three-layer ACSR conductor

R_1 - R_3: Resistance of aluminium layers
U_{i1} - U_{i3}: Induced voltage in aluminium layers
I_{AI} - I_{AII}: Induced current component in aluminium layers

The axial magnetic field of steel core induces voltages in aluminium layers. The direction of the induced voltage is opposite in middle-layer, because the stranding direction is opposite in middle layer comparing to the first and the third one. The absolute values of induced voltages depend on stranding geometry of the conductor.
The current in the middle layer caused by induced voltages increases the resultant current in the this layer, while the current decreases the resultant current of first and third layer. The current decreases the induction of the steel core and the iron loss, while causes increase-loss in aluminium layers.

According to the test results it was verified that the highest current density is not in the outside layer, caused by ”skin” effect, but in the middle-layer because of the transformer effect inducing current in the wires as a result of the magnetization of the steel core. The current density of the middle layer of a three layer ACSR conductor (500/65) is about 15-20 % higher than the average current density. The current density of layers depend on stranding geometry of conductors.

4.4 Loss calculation method of ACSR conductors taking into account the uneven current distribution.

The experiments have shown that the stranding geometry has a strong effect on the current distribution and axial magnetic field which cause the iron loss in the steel core and over-loss in the aluminium layers.
The uneven current distribution decreases the magnetic field strength in the steel core. The majority of over-loss develops in the aluminium layers, but not in the steel core.
On the basis of test results and theoretical study [5, 6,7, 8] it was shown, that the loss of ACSR conductors can be determined only by knowing the current distribution of AL-layers, therefore a new substitution connection of the stranded conductor with three layers was developed (Appendix A and Appendix B.)

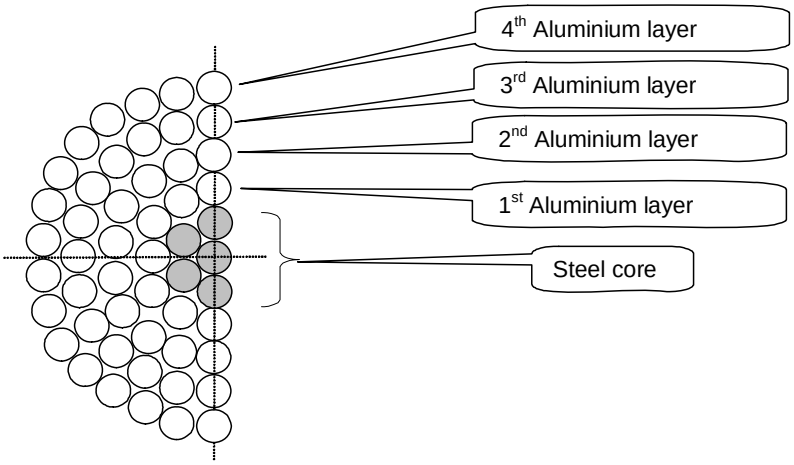

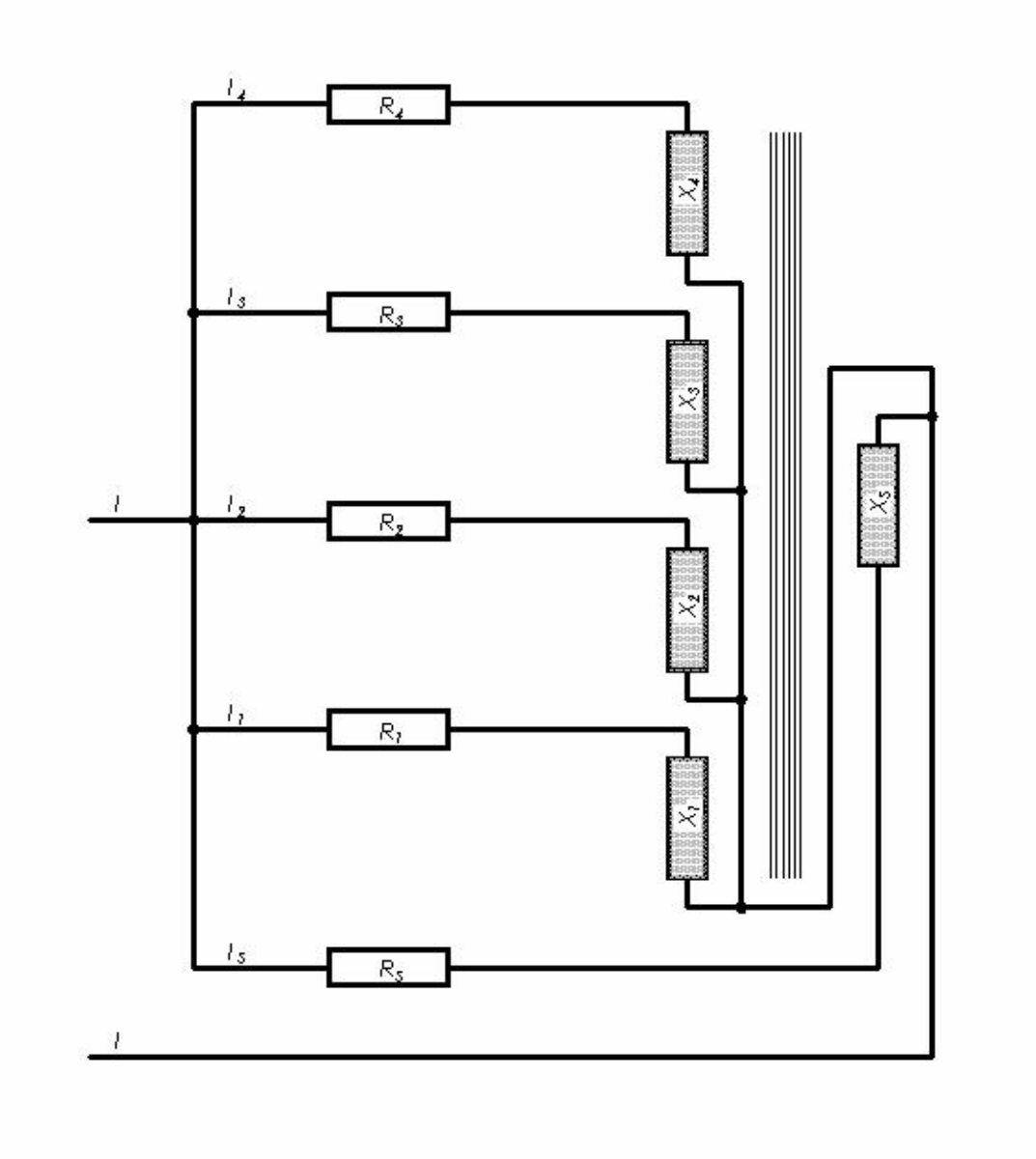

Fig 6: Electrical representation of three layer conductor as described in Appendix A.

The diagram shown in figure 6 represents the exact model used in the Mathcad model described in Appendix A. It is sufficiently accurate and the mathcad model takes into account the skin effect, eddy current and transformer effect. The diagram shown in Appendix B represents the exact model used in the computer program developed by Güntner and Varga. The model of Appendix B takes into account transformer effect, eddy current and histeresis losses of steel core, as well as the current and temperature distribution of aluminum layers.

The primary circuits substitute the aluminium layers while the secondary circuit substitutes the steel core. In the substitutions diagram "I" symbolises the current in the conductor, which is equal to the sum of the current in each layer(I1, I2,I3, I4.) The Figure 6 is equivalent to the model in [14] except that it combines the inductances from longitudinal and circular magnetic flux. In the reference [14], the two types of inductance are shown separately, with the

longitudinal inductances resulting in transformer effect and the circular inductance producing skin effect.

Some theoretical studies, [21,25,47] did not take into account the uneven current distribution of Al layers, therefore the increment of AC resistances consist of eddy-current, and hysteresis losses of steel-core.

The loss of the layers and the steel core can be determined on the basis of substitution connection diagram [5].

According to calculation, about 80% of AC incremental loss is produced in the Al-layers and only 20% of it arises in the steel-core. The variation of components (ΔRAl,and ΔRAc) of AC resistance of conductors can be seen in Fig. 7 (assuming no saturation of the steel core).

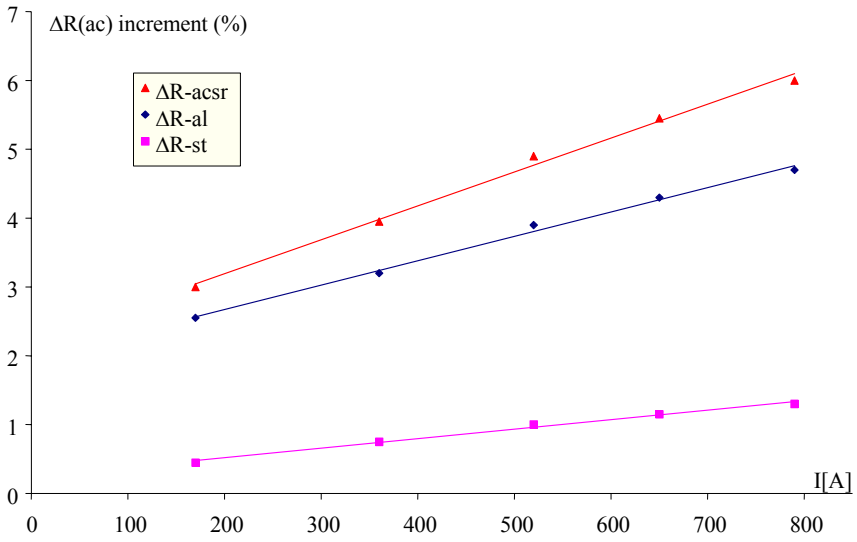

Fig. 7.
Main components of AC resistance

The cause of increase of AC resistance in comparison to the DC resistance, is mainly uneven current distribution, which strongly depends on the induced voltage in the Al-layers. This voltage is the function of the stranding angles of the layers.

According to laboratory test results, it can be established that a calculation method, which is capable to define the current distribution of Al-layers as a function of stranding angles [5,6,7, 8, 45, 46] is to be used for calculation of AC-resistance of ACSR conductors.

5 AC RESISTANCE CALCULATION OF ACSR CONDUCTORS

A computer program (format given in Appendix A) was used to calculate the AC resistance of ACSR conductor samples, with one layer and three layers construction.
The following conductors were used:

One layer conductors: Turkey, Raven, Penguin
Three layers conductors: Lapwing, Falkon

Geometrical parameters are shown in Table 1.

Table 1.Geometrical parameters of conductors

Type of Conductor	Area al / steel mm^2	Overall Diameter Mm	Number and diameter of wires n x mm		Lay ratio / angle of stranding			
			steel	Aluminium	Aluminium layers			Steel core
					Inner	middle	outer	
Turkey	13,3 / 2,2	5,04	1 x 1,68	6 x 1,68	13,5 / 81,2	_	_	- / 90
Raven	53,5 / 8,9	10,11	1 x 3,37	6 x 3,37	13,5 / 81,2	_	_	- / 90
Penguin	107,2 / 17,9	14,31	1 x 4,77	6 x 4,77	13,5 / 81,2	_	_	- / 90
Lapwing	804 / 56	38,16	7 x 3,18	(9+15+21) x 4,77	12,5 / 79,3	11,5 / 77,2	10,5 / 75,3	18 / 83,4
Falcon	806 / 102	39,26	19 x 2,62	(12+18+24) x 4,36	12,5 / 78,6	11,5 / 76,8	10,5 / 75,1	18 / 82,1

The calculated value of AC/DC resistance ratio of one layer and three layers conductor as a function of loading current are presented in Fig. 8.- 9.

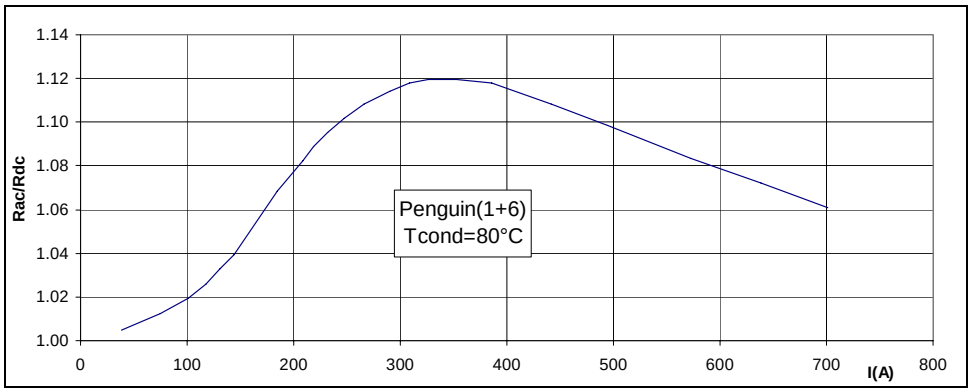

Fig. 8
Variation of AC/DC resistance of Penguin conductor

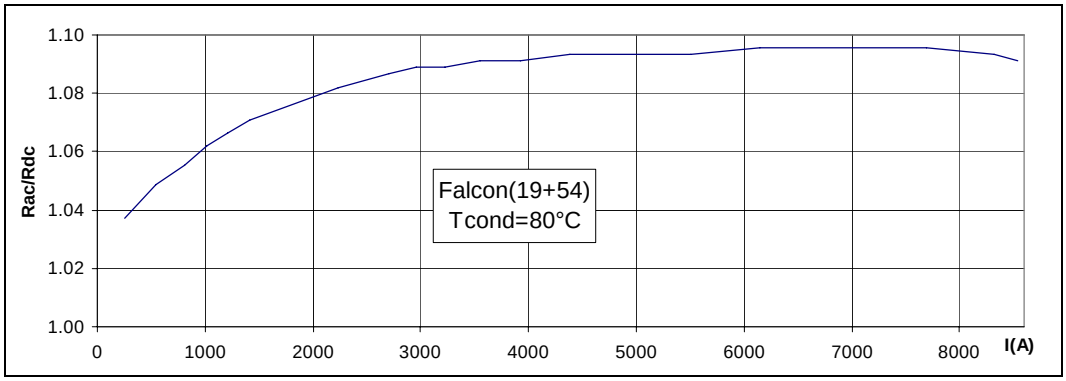

Fig. 9
Variation of AC/DC resistance ratio of Falcon conductor

The reader can clearly see two effects from these calculations:
The increase in ac resistance is not linear with current density. Rather, a peak resistance is reached at a current density of 3 to 5 amperes/mm^2 after which the resistance either flattens out or declines as a result of the saturation of the steel core.

The AC/DC resistance ratio of the larger Falcon conductor starts at about 4% even though the current density is very small. This indicates a conventional "skin effect" with such large conductor whether there is a steel core or not.

6 INFLUENCE OF CONDUCTOR STRANDING CONSTRUCTION ON RESISTANCE RATIO

The influence of stranding construction is shown for ACSR conductors of type 54/7 and 42/7 for a Lay Ratio of 13.5*D in Fig. 10.

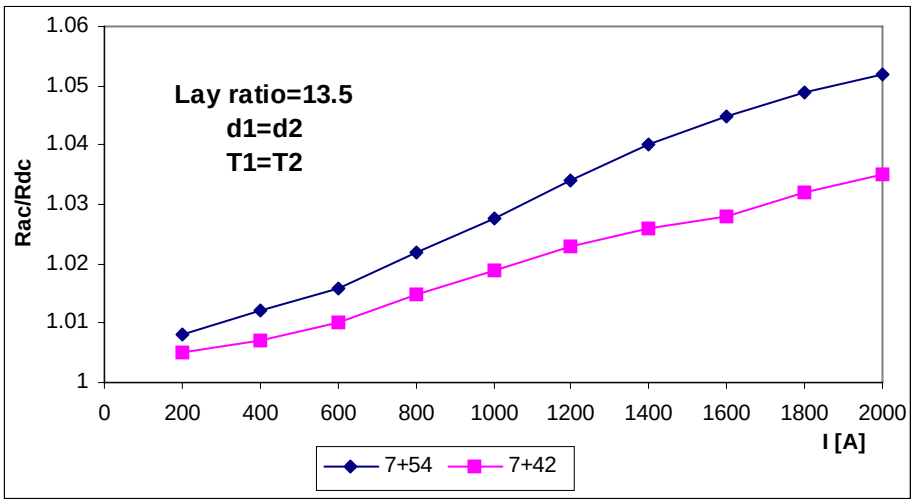

Fig. 10.
The influence of conductor stranding on AC/DC resistance ratio

For 54/7 ACSR conductors, the influence of wire diameter (Fig.11.) and temperature (Fig.12.) on resistance ratio are shown.

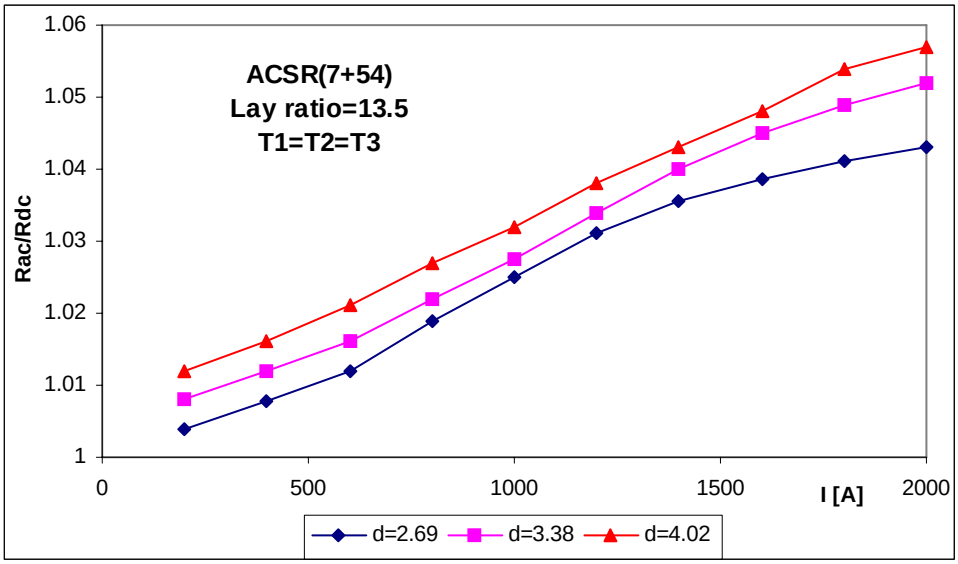

Fig.11.
The influence of wire diameter to the AC/DC resistance ratio

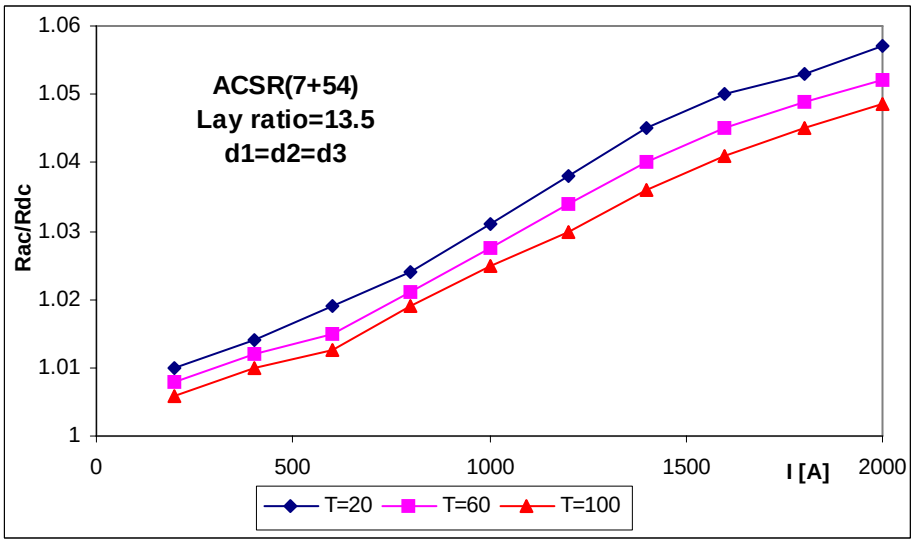

Fig. 12.
The influence of conductor temperature to the AC/DC resistance ratio

6.1 The effect of the lay ratio to the AC/DC resistance ratio

In calculating resistance ratios in the preceding figures, a lay ratio:of 13.5 was maintained. Any change of the lay ratio has significant impact on the AC resistance [5, 7]. This represents a limitation on accuracy if the lay ratio is not known.

As Fig.13. shows, differences in lay ratio between layers can yield a large impact on the resistance ratio. A typical ACSR conductor is compared to one whose lay ratios are adjusted to yield a minimum magnetic field in the steel core.

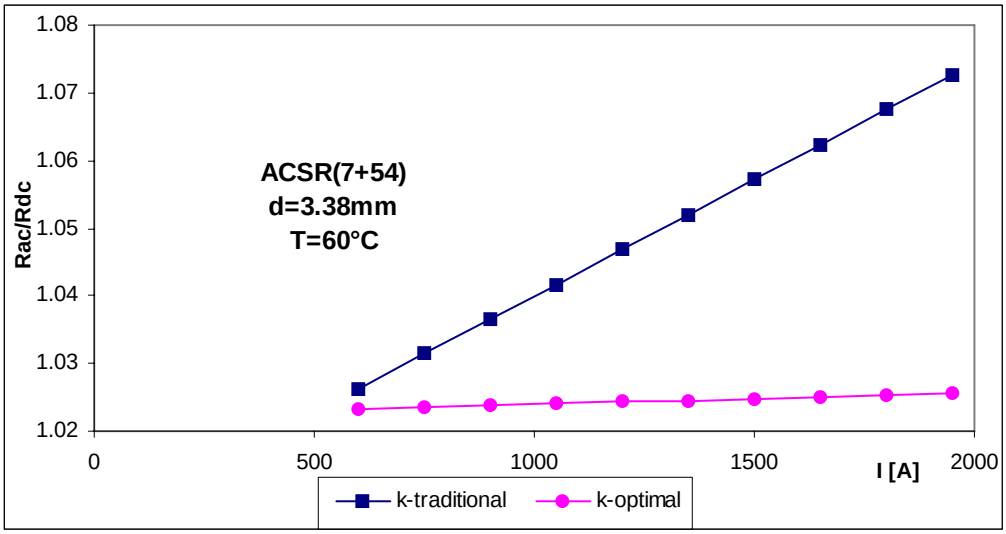

Fig. 13.

Ultimate difference of Rac/Rdc ratio between traditional and optimal stranding

7 COMPARISON OF MEASURED AND CALCULATED DC AND AC RESISTANCE VALUES

7.1 Comparison between the two models decribed in Appendices A and B.

A calculation method was developed by Muftic (Eskom) using the MathCad software based on [14]. This method was based on the model in Appendix A. Another computer program was developed by Güntner and Varga (VEIKI-VNL Ltd.) for AC resistance calculation. This program is based on the model shown in Appendix B.

Data of ACSR 500/66 conductor:

Steel core: 1+6 wires, 3.45 mm diameter
Alu layers: 12+18+24 wires, 3.45 mm diameter
Lay ratio of steel: 20
Lay ratio of Aluminum layer1 (outer): 12
Lay ratio of Aluminum layer2 (middle): 13
Lay ratio of Aluminum layer3 (inner): 14

The measured and the calculated values with two different methods can be seen in Fig. 14.

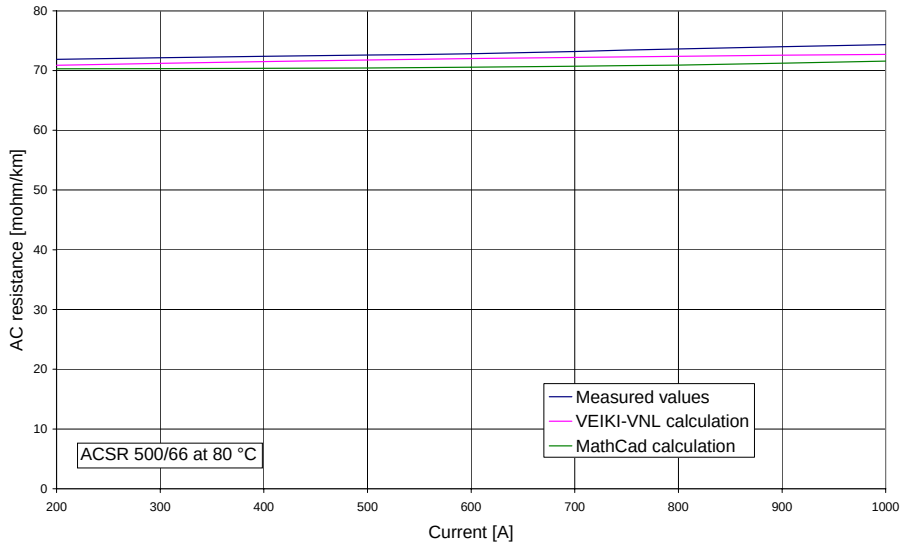

Fig. 14.
Measured and calculated results for ACSR 500/65 conductor

From the diagram it can be recognised that the two calculation programs give relatively the same results. From the diagram Fig 14. can be recognised too, that the measured AC resistance values are very closed to the calculated results with both of them computerprogram, based on the theory of uneven current and temperature distribution of ACSR conductors.

Note that some working group members consider the model in Appendix B to be unnecessarily complicated and feel that it has not been shown to be theoretically valid. Figures B2 and B3 illustrate current loops for the core that are isolated from te rest of the conductor. Core resitances occur three times in figure B2 and twice in figure B3. This does not correspond to the physical conductor, in which there is only one core resistance.

The diagram in A1 and figure 6 are considered by some to be superior in that the topology corresponds to that of the physical conductor as illustrated in [14].

7.2 Comparison between model in Appendix A and Barret and Morgan measured results

The following graphs indicate the comparison between the Barret and Morgan measured results using two and three layer conductors.

7.2.1 Two layer conductor

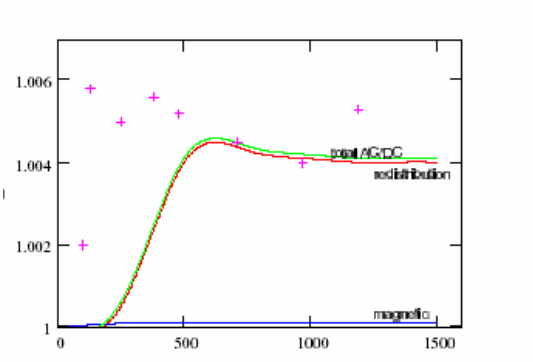

Figure 15 Comparision between Barret (+) and calculated results for a two layer conductor. (Grackle with outer layer removed)

The Figure 15 above shows the comparison between the Barret and calculated results. Note that the ratio is very cloe to unity hence the apparent large scatter which, in absolute terms is relatively small. The following table shows the component contribution making up the ratio.

Current (A)	Skin effect contribution	Current redistribution increment	Magnetic losses increment	Total AC/DC resistance ratio
0	0.000	0.000	0.000	1.000
250	0.004	0.0005	0.0001	1.0006
500	0.004	0.004	0.0001	1.0041
750	0.004	0.0043	0.0001	1.0044
1000	0.004	0.0041	0.0001	1.0042
1250	0.004	0.004	0.0001	1.0041
1500	0.004	0.004	0.0001	1.0041

Table showing the components of the ratio.

7.2.2 Three layer conductor

The following graph shows the comparison between Barret (+), Morgan (x) and the calculated values for a Grackle conductor as a function of current.

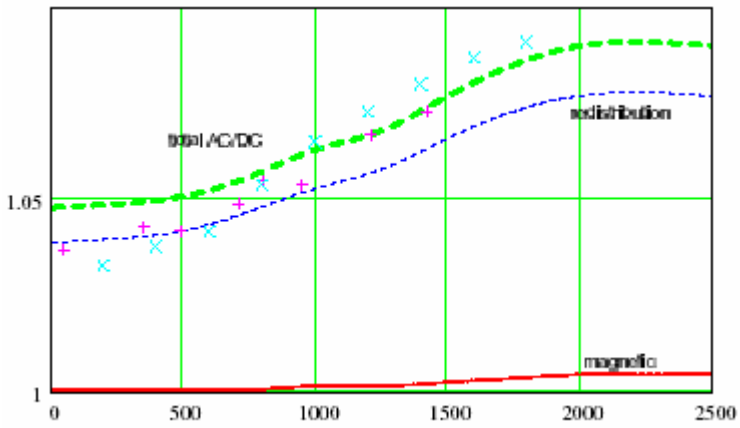

Fig 15 showing the AC/DC resistance ratio as a function of current for Grackle conductor.

The above figure indicates the accuracy of the model in relation to the three layer conductor. The accuracy is considered acceptable when compared to previous measured results.

The following table shows the component of the AC/DC ratio.

Current (A)	Skin effect contribution	Current redistribution increment	Magnetic losses increment	Total AC/DC resistance ratio
0	0.000	0.000	0.000	1.000
250	0.008	0.040	0.001	1.049
500	0.008	0.042	0.001	1.051
750	0.008	0.047	0.001	1.056
1000	0.008	0.053	0.002	1.063
1250	0.008	0.058	0.002	1.068
1500	0.008	0.066	0.003	1.077
1750	0.008	0.073	0.004	1.085
2000	0.008	0.077	0.005	0.090
2250	0.008	0.078	0.005	0.091
2500	0.008	0.077	0.005	0.090

Table showing the components of the ratio.

8 CONCLUSION

The theory surrounding the current distribution in stranded conductors is well researched and documented. Prior to the advent of modern day mathematical programmes, it was not possible to rapidly calculate the AC resistance value in a short time. This necessitated simplification of the detailed model to allow engineers to determine approximate values of AC resistance. This sufficed whilst the current densities used were generally well below 1A/mm^2. However, in recent time with the pressure to relieve conjestion due to trading and other factors being prevalent, current densities of up to 4 A/mm^2 have been experienced. This implies that the present simplification is not sufficient. This document has managed to describe the model relating to the determination of AC resistance as well as indicate the comparison of the use of the model to actual measurements. The example of more generalised model [50] in Appendix
A allow the user to develop programmes to determine the AC resistance of any conductor type.

In the version of mathcad described in Appendix A the temperature per layer will be considered as an input from main algorithm of steady state calculation . When program is used as a stand alone, for the purpose of analysis of AC/DC ratio for example, the uniform temperature distribution can be asuumed.

The calculation method and flowchart of the computer program developed by Güntner and Varga [5, 6, 7, 8] are in Appendix B. By using the computer program and theory described in Appendix B the AC and DC resistance as well as the temperature rise and current distribution of ACSR conductors can be determined.

The use of the theory was further developed to indicate the possible design of a conductor to eliminate the effect of current on resistance.

From these studies it can be recognised that the calculation method, based on the theory of uneven current and temperature distribution of aluminum layers is acceptable for determination of AC resistance of ACSR conductors.

The simplified methods used previously should not be used at high current densities. It is preferable that the model developed in this document be used to accurately determine the AC resistance in revised CIGRE conductor temperature steady state mathematical model.

9 REFERENCES

[1] E.H. Salter, Problems in the measurement of AC resistance and reactance of large conductors", AIEE Trans., Vol. 67, Part II, pp. 1390-1397, 1948.

[2] A.H.M. Arnold, "The alternating-current resistance of parallel conductors of circular cross-section", Jour. IEE, Vol. 77, pp. 49-58, 1935.

[3] F. Castelli, "Four-terminal impedance current transformer bridge with resistive ratio arm", IEEE Trans.Power Appar. Syst., Vol. 98, No. 3, pp. 972-981, 1979.

[4] P.E. Burke and R.T.H. Alden, "Current density probes", IEEE Trans. Power Appar. Syst., Vol. 88, No. 2, pp. 181-185, 1969.

[5] Ottó Güntner: The effects of the uneven current distribution within the aluminium layers on the losses of ACSR OHL conductors.
Dissertation, 1989, Technical University of Vienna.

[6] O.Güntner- Gy.Danyek: Computer aided design of optimised stranded conductors. Acta Technica Acad. Sci. Hung. 105(1-2) pp. 19-40(1993).

[7] László Varga: The determination method of allowed loading current of overhead line onductors.
Dissertation, 1990, Budapest Hungarian Academy of Science.

[8] László Varga: Determination of the current distribution and current load of overhead line conductors.
Acta Technica Acad. Sci. Hung. 105(1-2) pp. 117-128, 1993).

[9] Morgan, V.T.: The thermal rating of overhead line conductors. Part II. Elect. Power Syst., 6 (1983), 287-300

[10] Black, Collins,: Theoretical model for temperature gradients within bare overhead conductors. IEEE Trans. on Pow. Det. 3, No. 2 (1988), 707-715

[11] Dzevad Muftic: AC/DC resistance ratio in the steady state ampacity calculation, Johannesburg, 1993

[12] V. T. Morgan - D. K. Geddey: Temperature distribution within ACSR conductors

[13] V.T.Morgan: Temperature distribution within ACSR conductors
CIGRE September. 1992. Paris.

[14] J.S. Barrett, O. Nigol, C.J. Fehervari and R.D. Findlay, "A new model of AC resistance in ACSR conductors", IEEE Trans. Power Delivery, Vol. 1, No. 2, pp. 198-207, 1986.

[15] V.T. Morgan, B. Zhang and R.D. Findlay, " Effect of magnetic induction in a steel-cored conductor on current distribution, resistance and power loss", IEEE Trans. Power Delivery, Vol. 12, No. 3, pp. 1299-1306, 1997.

[16] F. Jakl and M. Žunec, "Distribution of current density in layers of overhead bare conductors", Proc. Inter. Conf. on Power Systems and Communications Systems Infrastructures for the Future, Beijing, China, September 23-27, 2002.

[17] J.C. Maxwell, *A Treatise on Electricity and Magnetism*, Constable, London, 1873.

[18] O. Heaviside, "Effective resistance and inductance of a round wire", Electrical Papers, Vol. 1, pp. 353, 429; Vol. 2, pp. 50, 97, 1994.

[19] V.T. Morgan, R.D. Findlay and S. Derrah, "New formula to calculate the skin effect in isolated tubular conductors at low frequencies", Proc. IEE-Sci. Meas. Technol., Vol. 147, No. 4, pp. 169-171, 2000.

[20] A.H.M. Arnold, "Copper losses in large cables at power frequencies", Jour. IEE, Vol. 76, pp. 299-322, 1935.

[21] W.A. Lewis and P.D. Tuttle, "The resistance and reactance of aluminum conductors, steel reinforced", AIEE Trans., Vol. 77, Part III, pp. 1189-1215, February 1959.

[22] C. Manneback, "An integral equation for skin effect in parallel conductors", Jour. Math. Phys., Vol. 1, pp. 123-146, 1922.

[23] A.H.M. Arnold, “Proximity effect in solid and hollow round conductors”, Jour. IEE, Vol. 88, Part II, pp. 349-359, 1941.
[24] V.T. Morgan and C.F. Price, “Magnetic properties in axial 50 Hz fields of steel core wire for overhead-line conductors”, Proc. IEE, Vol. 116, No. 10, October 1969.
[25] V.T. Morgan, “Electrical characteristics of steel-cored aluminium conductors”, Proc. IEE, Vol. 112, No. 2, pp. 325-334, February 1965.
[26] V.T. Morgan The current-carrying capacities of overhead-line conductors”, Proc. IEEEPower Engineering Society Summer Meeting, Los Angeles, CA, July 1978, Paper A78 575-3, 18 pp.
[27] J.A. Clegg, “Tests on the electric and magnetic properties of aluminium-steel cored cable”, Jour. IEE, Vol. 77,pp. 59-62, 1935.
[28] R. Goldschmidt, “The resistance of aluminium-steel cables to alternating current”, CIGRE Paris, Paper 214, 1952.
[29] K.R. Malayan, Calculation of the effective resistance of steel-aluminium conductors at power frequency”, Akad. Nauk Armyansk. SSSR. Izvest. Ser. tekh. Nauk, Vol. 24, No. 2, pp. 58-66, 1971.
[30] R.D. Findlay and D.T. Jones, “Modeling technique for single-layer conductors with steel reinforcing”, IEEE Power Engineering Society Summer Meeting, Portland, Oregon, July 1976, Paper A76-434-1.
[31] R.D. Findlay, “Equivalent nonlinear lumped parameter network representations for ACSR conductors”, Proc. IEE, Vol. 127C, No. 6, pp. 430-433, 1980.
[32] J. Zaborszky, “Skin and spiraling effect in stranded conductors” AIEE Trans., .Vol. pp. 599-603, August 1953,
[33] V.T. Morgan, B. Zhang and R.D. Findlay”, Effectsn of temperature and tensile stress on the magnetic properties of a steel core from an ACSR conductor, IEEE Trans., Power Delivery, Vol. 11, No. 4, pp. 1907-1913, October 1996.
[34] V.T. Morgan, R.D. Findlay and B. Zhang, “Distribution of current density in ACSR Conductors”, Proc. Canadian Conf. On Electrical and Computer Engineering, Halifax, NS, September 1994, pp. 165-168.
[35] A.Russell, *Alternating Currents*, Vol. 2, Cambridge, 1914, p. 224.
[36] V.T. Morgan, “Effects of alternating and direct current, power frequency, temperature and tension on the electrical parameters of ACSR conductors”, IEEE Trans. Power Delivery, accepted for publication, 2003.
[37] V.T. Morgan and R.D. Findlay, “The effect of frequency on the resistance and internal inductance of bare ACSR conductors”, IEEE Trans., Power Delivery, Vol. 6, No. 3, pp. 1319-1323, July 1991.
[38] V.T. Morgan, “The radial temperature distribution and effective radial thermal conductivity in bare solid and stranded conductors”, IEEE Trans., Power Delivery, Vol. 5, No. 3, pp. 1443-1452, July 1990.
[39] D.A. Douglass, “Radial and axial temperature gradients in bare stranded conductors”, IEEE Trans., Power Delivery, Vol. 1, No. 2, pp. 7-15, April 1986.
[40] Zarebski, W.: Obciaualnosc pradoeva prezewodow linij napowietrznich Biuletin Institut Energetyki ,1968, 3/4, (Warsaw, 24-47
[41] Nicholson, I.: Influence of conductor designs and operating temperature on the economy of overhead lines. Proc. IEEE, 118, No. 3/4 (1971)
[42] Webs, A.: Dauerstrombelastbarkeit von nach DIN 48201 gefertigten Freileitungsseilen aus Kupfer,
Aluminium und Aldrey. Elektrizitätswirtschaft 23 (1963), 861-872

[43] Morgan, V.T.: Some factors which influence the continuous and dynamic thermal rating of overhead line conductors.
CIGRE Symposium 06-85, Brussels 1985, 1-6

[44] V.T. Morgan: Electrical characteristics of steel-cored aluminium conductors PROC, IEEE. Vol. 112. No. 2. February, 1965.

[45] Barret- Findlay: A new model of AC resistance in ACSR conductors, IEEE. Trans., Vol. PWRD.-1, No. 2, 198-208 (April, 1986)

[46] Barret, J. S.: Optimisation of conductor design.
IEEE. Trans., Pow., Vol. 4, No. 1. (January, 1989)

[47] Match - Luis.: The magnetic properties of ACSR core wire IEEE. TRANS. / 1959.

[48] Tóth-Güntner-Varga: Problems of the short circuit strength of overhead lines, CIGRE 1977. WG 31-02.

[49] Dr. Franc Jakl: Investigations of thermal and mechanic characteristics of bare conductors under short-circuit conditions
CIGRE SC 22 WG 12 1994 JAPAN.

[50] Dzevad Muftic: AC resistance in the steady state ampacity calculation, contribution to the book: PLANNING, DESIGN AND CONSTRUCTION OF OVERHEAD POWER LINES (ESKOM, , Johannesburg, February 2005)

10 NOMENCLATURE

A	Cross-sectional area
A_s	Cross-sectional area of steel core
d	diameter of each ~~cube~~wire
d_a	diameter of aluminum core
d_s	diameter of steel core
D_s	outside diameter of conductor
D_n	mean diameter of layer n
D_p	mean diameter of layer p
f	frequency
h_i	pitch of aluminum wires in layer ~~2~~i
i	index (1, 2 ….) of layer
J	number of conductor layers
k_1	constant
k_2	constant
n	number of conductor layers
n_a	number of aluminum layers
n_s	number of steel layers
N	effective number of turns per unit length
R	Resistance per unit length of conductor
R_1-R_3	Resistance of aluminum layers
R_{dc}	DC resistance per unit length of solid cylindrical conductor
R_s	DC resistance of steel core
T	Temperature of conductor
V_s	Voltage drop per unit length in steel layer
V_1-V_3	Voltage drop per unit length in aluminum layers
ω	Angular frequency (r~~v~~ad/s)
X_{nn}-X_{ss}	Complex self impedance
X_{pq}	Complex mutual impedance
$X_{n,\ inner}$	inner mutual indicative reactance due to inner flux
$X_{n,\ outer}$	outer mutual indicative reactance due to outer flux
α_{20}	Temp coefficient at 20°C
δ	Phase angle between total current and voltage indeed in non-ferrous wires
ΔR	Resistance increase
λ_I	lay length of layer i
λ_n	lay length of layer n
λ_p	lay length of layer p
$\lambda_{~~q~~i}$	lay length of layer q
μ_o	permeability of free space
μ_r	complex relative permeability of the core
ϱ	Resistivity
ϱ_{20}	Resistivity at ~~of~~ temperature of 20°C
ϱ_a	resistivity of aluminum
ϱ_s	resistivity of steel
$\downarrow$	Phase angle between loading current and voltage induced in the aluminum layer
$\downarrow_{n,\ inner}$	inner magnet flux associated with layer n
$\downarrow_{n,\ outer}$	outer magnet flux associated with layer n

APPENDIX A

a. Explanation of computer programme to calculate the AC resistance for a particular current

This program was developed in MatCad, but can be easily transformed to any other commonly used languages. It assumes a full and comprehensive mathematical model based on works of Morgan, Barrett, Varga and others. One of important features here is treating a permeability curve as an input. It means, whenever more reliable/accurate information from lab measurement are available, originally assumption based on curve given by Barrett can be easily replaced. Also, coefficients which describe displacement of current from the center of wire (kio and 1- kio, in (16) above) are input which can be changed according to specific findings/experience). The geometry of the conductor can be any associated with a helically stranded conductor. It can be also be any composition of AAAC, ACSR, ACAR conductor. The total number of layers, however, is limited to 7, which is sufficient for present practice. However, it is a simple matter to increase this limit should such a requirement arise. First layer is always considered to be first wire in the center of conductor.

Magnetic core loss increment was calculated using Morgan's formula at the end of program only as an example. The magnetic core loss should be calculated within the same thermal rating algorithm once current distribution and temperature distribution are known (iterative process in CIGRE thermal model).

The schematic diagram of three layer conductor is represented in Fig A/1.

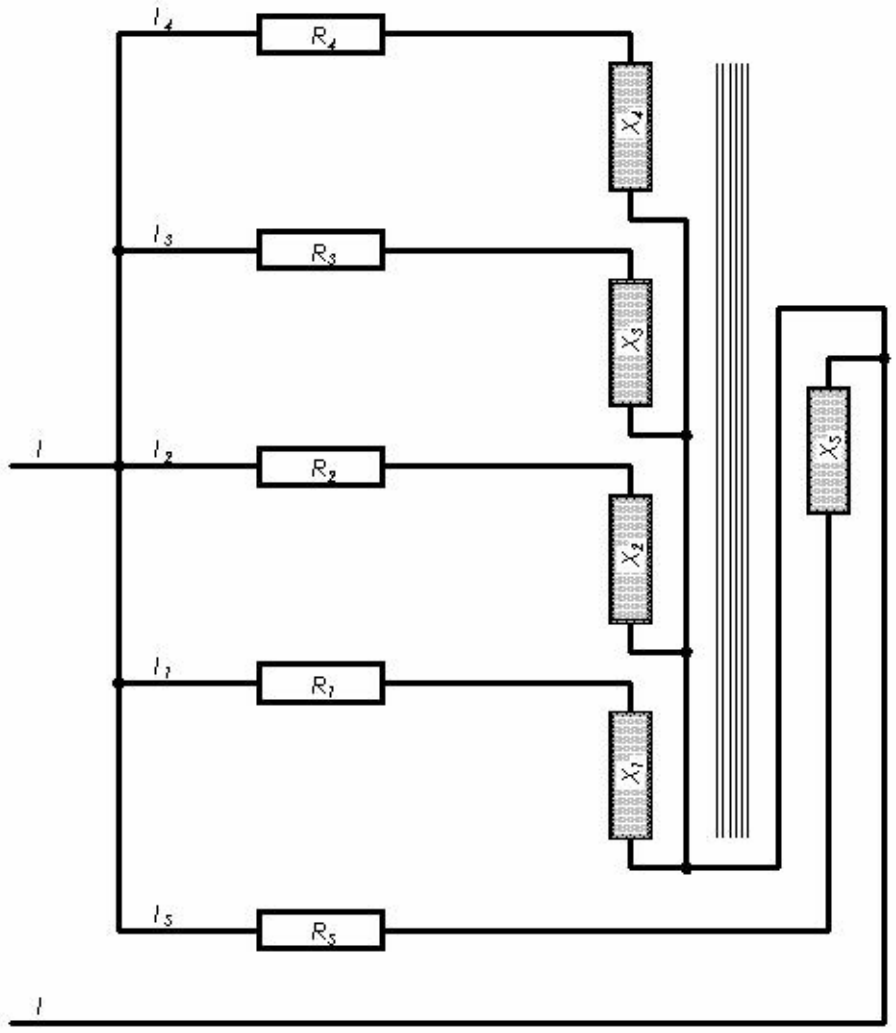

Fig. A/1
Schematic diagram of three layers conductor

b. Equations of AC resistance calculation method for Mathcad model

The set of equations which gives voltage drop in each individual layer can be given as follows based on figure 6b,

Vs = Is [Rs – j Xss+ kio j Xcss] + I1 (j Xs1 + Xcs1) + I2 (-j Xs2 + j Xcs2) +
I3 (j Xs3 + j Xcs3) + I4 (- j Xs4 + j Xcs2) (A/1)

V1 = Is [- jX1s+ (1- kio) j Xc1s] + I1 [R1 + j X11+ kio j Xc11] + I2 (- j X12 + j Xc12)+ I3 (j X13 + j Xc13) + I4 (- j X14 +j Xc14) (A/2)

V2 = Is [-j X2s+ (1- kio) j Xc2s] + I1 [j X21 + (1- kio) j Xc21] + I2 [R2 - j X22+ kio j Xc22] +I3 (j X23 + j Xc23) + I4 (- j X24 + j Xc24) (A/3)

V3 = Is [-j X3s+ (1- kio) j Xc3s]+ I1 [jX31+ (1- kio) j Xc31] + I2 [- j X32 +(1- kio) j Xc32] +I3 (R3 + j X33 + kio j Xc33) + I4 (- j X34 + j Xc34) (A/4)

V4 = Is [-j X4s+ (1- kio) j Xc4s]+ I1 [jX41+ (1- kio) j Xc41] + I2 [- j X42 +(1- kio) j Xc32] + I3 [j X43 + (1- kio) j Xc43] + I4 [R4 - j X44+ kio j Xc44] (A/5)

Please note that a negative value on even number of layers is result of opposite stranding comparing to uneven number.

The sum of layer currents must equal total current I:

$I = I_1 + I_2 + I_3 + I_s$ (A/6)

The voltage drop of each layer is equal:

V = V1 = V2 = V3 = Vs (A/7)
This includes the Vs for all layers of steel.
.
From the calculated layer currents we can get the voltage drop and then calculate the AC resistance as:

R_{AC}= Re (V / I) (A/8)

Although looks a little bit complicated, it can be solved rather easy using presently available tools.

Using the algorithm explained above a program for calculation of AC/DC ratio (current redistribution increment) was developed.

The programme shown in this appendix does the following:-

Note that an assumption is made as to the current flowing. The program then calculates the magnetic heating component P_m which is then substituted back into the heat balance equation to determine a new current.

Input data – the data relating to the geometry of the conductor is entered. The example given is that of Grackle although any conductor of any material can be entered.

INPUT General Data

Frequency, magnetic permeability of the air, specific resistance of various materials used for conductor construction (exp: steel, aluminum alloy, aluminum etc)
Assign a code number to materials (exp: steel Code 1, aluminum alloy Code2, aluminum Code 3 etc)

INPUT Conductor Geometry

Number of core layers, number of outer layers (total number of layers not to exceed 7)

Starting with the inner most layer, specify material code, number of wires, diameter of wires in mm and lay ratio

Calculate AC Current distribution by iteration.

A geometry summary is then calculated which includes the lengths of strands and diameters of each layer and areas of steel and aluminium.

OUTPUT conductor geometry matrices:
Material code, specific resistance , number of wires in each layer, outer diameter of each layer, lay ratio and lay length

OUTPUT A (cross sectional area) matrix and As (steel core cross sectional area) matrix and At (total cross sectional area of conductor) and As (total steel core cross sectional area)

The DC resistance is then calculated per layer.
An assumption is made as to the current and the current distribution as a result of different strand lengths is calculated.

Calculate DC resistance matrix for each layer using DC resistance equation and total conductor DC resistance

Calculate DC current distribution assuming I_{tot}= 1000 Amps and also DC voltage drop matrix

The relative permeability is then calculated from the electric field strengths and reading the real and imaginary component off the curves (representative laboratory test results). These curves can be entered by the user and the programme has indicated these curves used originally by Baret at al [14].

Perform Electric Field , Relative Permeability calculations assigning signs to each layer
SGN is used as the identification of direction of stranding ensuring that + sign is always associated with righ-hand direction and – with opposite. Also, small algorhitm ios her eto ensure that first layer (steel or al is always in right direction.
Calculate H. (assuming λ_0=1000, there is confusion here as λ_0 is also lay length. Also λ_0 is 0, so how is Hh calculated for i=0 layer
λ_0=1000 is used here as an equivalent to λ_0=indefinite, notice in new wersion of program this confusion is eleiminated by introducing correct indefinite value.

The reactance matrix is then determined.

Calculate Reactance Matrix:

. It is calculated exactly according to the formula gigiven for Xi,j doung all permutations for I and j example is given for the same Grackle which is going all the way through a whole program
INPUT current displacement assumption was assumed here as an input just to allow the change if thre is better knowledge of that than what Baret and Morgan have given.

The circular flux reactance is then determined

Calculate circular Flux Reactance: (again a sample entry calculation would add value dm: the same princilple and similar example like for reactance matrix) Process and nomenclature clarification is required here. Flux matrix is calculated.

From these two matrices, the impedance matrix can be determined.

Calculate Impedance matrix (again a typical entry calculation would help given, dm)

Calculate AC Current distribution by iteration.

The AC current distribution is then calculated for each layer by solving the matrix eqation:

$$[I] = [V] / [Z]$$

The calculation of new electric field and corresponding relative magnetic permeability is than repeated until the the balance of assumed total current (input) and calculated current is reached. Here, it was done in the loop of max 24 steps. Tests proved that results are converging to the expected balance much below this number of loops.

From these results the AC resistances are determined.

Calculate Ac Resistance matrix Result $_{0,0.}$:
Result $_{0,0.}$ - current vector Ip
Result $_{0,1}$ - impedance matrix Z
Result $_{0,2}$ - electric field vector Hh
Result $_{0,3}$ - total electric field strength H
Result $_{0,4}$ - voltage drop vector ΔV

The programme also calculates the actual R_{ac}, the AC/DC ratio (current redistribution component), the magnetic field B_m and hence the P_m.

This is not the final value but now needs to be placed in the heat balance equation from which a new value of Pm will be determined. This value will result in a different current which then needs to go back into the loop.

c. Math Cad code for AC resistance calculation

PROGRAM FOR CALCULATION OF AC RESISTANCE OF HELICALLY STRANDED CONDUCTORS

GENERAL INPUT DATA:

$f := 50$ Hz - frequency

$\mu_0 := 4 \cdot \pi \cdot 10^{-7}$ - magnetic permeability of the air

$\rho st := 0.1775$ $\frac{\Omega \cdot mm^2}{m}$ - specific resistance of steel, Code 1

$\alpha st := 0.00393$ $\frac{1}{degC}$ - temperature coefficient of steel

$\gamma st := 7.78$ $\frac{kg}{dm^3}$ - density of steel

$\rho aal := 0.0327$ $\frac{\Omega \cdot mm^2}{m}$ - specific resistance of alloy, Code 2

$\alpha aal := 0.00360$ $\frac{1}{degC}$ - temperature coefficient of alloy

$\gamma all := 2.7$ $\frac{kg}{dm^3}$ - density of alloy

$\rho al := 0.028126$ $\frac{\Omega \cdot mm^2}{m}$ - specific resistance of aluminium, Code 3

$\alpha al := 0.00404$ $\frac{1}{degC}$ - temperature coefficient of aluminium

$\gamma al := 2.7$ $\frac{kg}{dm^3}$ - density of aluminium

CONDUCTOR GEOMETRY DATA:

example: Grackle ACSR

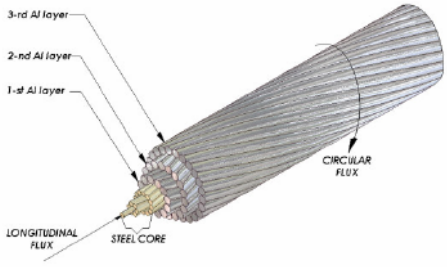

$Nls := 3$ - number of steel layers

$Nlaa := 0$ - number of alloy layers

$Nla := 3$ - number of aluminium layers

$Nl := Nls + Nlaa + Nla$ $Nl = 6$ - **total number of layers** (limited to 7)

$Mc_0 := 1$ - material code of 1st layer (first wire in centre assumed as 1st layer)

$nw_0 := 1$ $dw_0 := 2.24$ - number and diameter (mm) of wires in 1st layer

$Layratio_0 := 0$ - lay ratio of 1st layer

$Mc_1 := 1$ - material code of 2nd layer

$nw_1 := 6$ $dw_1 := 2.24$ - number and diameter (mm) of wires in 2nd layer

$Layratio_1 := 29.21$ - lay ratio of 2nd layer

$Mc_2 := 1$ - material code of 3rd layer

$nw_2 := 12$ $dw_2 := 2.24$ - number and diameter (mm) of wires in 3rd layer

$Layratio_2 := 16.58$ - lay ratio of 3rd layer

$Mc_3 := 3$ - material code of 4th layer

$nw_3 := 12$ $dw_3 := 3.78$ - number and diameter (mm) of wires in 4th layer

$Layratio_3 := 15.55$ - lay ratio of 4th layer

$Mc_4 := 3$ - material code of 5th layer

$nw_4 := 18$ $dw_4 := 3.78$ - number and diameter (mm) of wires in 5th layer

$Layratio_4 := 14.05$ - lay ratio of 5th layer

$Mc_5 := 3$ - material code of 6th layer

$nw_5 := 24$ $dw_5 := 3.78$ - number and diameter (mm) of wires in 6th layer

$Layratio_5 := 13.82$ - lay ratio of 6th layer

$Mc_6 := 0$ - material code of 7th layer

$nw_6 := 0$ $dw_6 := 0$ - number and diameter (mm) of wires in 6th layer

$Layratio_6 := 0$ - lay ratio of 7th layer

Geometry, summary:

$i := 0 .. NI - 1$

$MatCod_i := Mc_i$

$NumWir_i := nw_i$

$DiaWir_i := dw_i$

$LayRat_i := Layratio_i$

$$\rho_i := \begin{cases} \rho st & \text{if } MatCod_i = 1 \\ \rho aal & \text{if } MatCod_i = 2 \\ \rho al & \text{if } MatCod_i > 2 \\ 0 & \text{otherwise} \end{cases}$$

$$\alpha_i := \begin{cases} \alpha st & \text{if } MatCod_i = 1 \\ \alpha aal & \text{if } MatCod_i = 2 \\ \alpha al & \text{if } MatCod_i > 2 \\ 0 & \text{otherwise} \end{cases}$$

$MatCod = \begin{pmatrix} 1 \\ 1 \\ 1 \\ 3 \\ 3 \\ 3 \end{pmatrix}$ - code of material, per layer

$\rho = \begin{pmatrix} 0.178 \\ 0.178 \\ 0.178 \\ 0.028 \\ 0.028 \\ 0.028 \end{pmatrix}$ - specific resistance, per layer

$\alpha = \begin{pmatrix} 3.93 \times 10^{-3} \\ 3.93 \times 10^{-3} \\ 3.93 \times 10^{-3} \\ 4.04 \times 10^{-3} \\ 4.04 \times 10^{-3} \\ 4.04 \times 10^{-3} \end{pmatrix}$ - temperature coefficient of resistance

number of wires per layer:

$NumWir = \begin{pmatrix} 1 \\ 6 \\ 12 \\ 12 \\ 18 \\ 24 \end{pmatrix}$

$$D_i := \begin{cases} dw_i & \text{if } i < 1 \\ D_{i-1} + 2 \cdot dw_i & \text{if } i > 0 \\ 0 & \text{otherwise} \end{cases}$$

$\lambda_i := Layratio_i \cdot D_i$

$D = \begin{pmatrix} 2.24 \\ 6.72 \\ 11.2 \\ 18.76 \\ 26.32 \\ 33.88 \end{pmatrix}$ - diamete of each layer (mm)

lay ratio per layer:

$LayRat = \begin{pmatrix} 0 \\ 29.21 \\ 16.58 \\ 15.55 \\ 14.05 \\ 13.82 \end{pmatrix}$

lay length (mm) per layer:

$\lambda = \begin{pmatrix} 0 \\ 196.291 \\ 185.696 \\ 291.718 \\ 369.796 \\ 468.222 \end{pmatrix}$

$A_i := nw_i \cdot \frac{\pi}{4} \cdot (dw_i)^2$

$A = \begin{pmatrix} 3.941 \\ 23.645 \\ 47.29 \\ 134.665 \\ 201.997 \\ 269.33 \end{pmatrix}$ - cross-section of each layer

$At := \sum A$ $\quad At = 680.868$ - **total area of conductor** (mm^2)

DC RESISTANCE CALCULATION:

$tc := 80$ - average temperature (C) of conductor; assumption

$t_i := tc$

$t = \begin{pmatrix} 80 \\ 80 \\ 80 \\ 80 \\ 80 \\ 80 \end{pmatrix}$ - temperature (C) per layer; first assumption

$$R20_i := \begin{cases} \frac{\rho_0}{A_0} & \text{if } i < 1 \\ \frac{\rho_i}{A_i} \cdot \sqrt{1 + \left(\pi \cdot \frac{D_i - dw_i}{\lambda_i}\right)^2} & \text{if } i > 0 \\ \infty & \text{otherwise} \end{cases}$$

$$Rdc_i := \begin{cases} \frac{\rho_0}{A_0} \cdot \left[1 + \alpha_0 \cdot (t_0 - 20)\right] & \text{if } i < 1 \\ \frac{\rho_i}{A_i} \cdot \left[\sqrt{1 + \left(\pi \cdot \frac{D_i - dw_i}{\lambda_i}\right)^2}\right] \cdot \left[1 + \alpha_i \cdot (t_i - 20)\right] & \text{if } i > 0 \\ \infty & \text{otherwise} \end{cases}$$

$$Rcon := \frac{1}{\sum \left(\frac{1}{Rdc}\right)}$$

$R20 = \begin{pmatrix} 0.045 \\ 7.526 \times 10^{-3} \\ 3.796 \times 10^{-3} \\ 2.116 \times 10^{-4} \\ 1.418 \times 10^{-4} \\ 1.065 \times 10^{-4} \end{pmatrix}$

$Rdc = \begin{pmatrix} 0.056 \\ 9.301 \times 10^{-3} \\ 4.692 \times 10^{-3} \\ 2.628 \times 10^{-4} \\ 1.761 \times 10^{-4} \\ 1.324 \times 10^{-4} \end{pmatrix}$ - DC resistance (Ω/m) per layer

$Rcon = 5.75516 \times 10^{-5}$ - total DC resistance of conductor (Ω/m)

```
Rep := | Dsteel ← 0
       | Dal ← 0
       | Dall ← 0
       | Asc ← 0
       | Aall ← 0
       | Aal ← 0
       | Rsteel ← 0
       | Rall ← 0
       | Ral ← 0
       | for i ∈ 0.. Nl − 1
       |     Dsteel ← Di  if MatCodi = 1
       |     Asc ← Ai + Asc  if MatCodi = 1
       |     Asc ← Asc
       |     Rsteel ← 1/Rdci + Rsteel  if MatCodi = 1
       |     Dall ← Di  if MatCodi = 2
       |     Aall ← Ai + Aall  if MatCodi = 2
       |     Rall ← 1/Rdci + Rall  if MatCodi = 2
       |     Rall ← Rall
       |     Dal ← Di  if MatCodi = 3
       |     Aal ← Ai + Aal  if MatCodi = 3
       |     Ral ← 1/Rdci + Ral  if MatCodi = 3
       | (Dsteel Asc Rsteel Dall Aall Rall Dal Aal Ral)
```

Summary of input data for skin effect calculation:

Dstou := Rep0,0 — Dstou = 11.2 — **- outer diameter of Al** (mm)

Dallou := Rep0,3 — Dstin := 0 — **- inner diameter of Al** (mm)

Dallin := | Dstou if Dallou > 0 | 0 otherwise — Dallou = 0 — **- outer diameter of Al** (mm)

Dalou := Rep0,6 — Dallin = 0 — **- inner diameter of Al** (mm)

Dalin := | Dstou if Dalou > 0 | Dallou if Dallou > 0 | 0 otherwise — Dalou = 33.88 — **- outer diameter of Al** (mm)

Asc := Rep0,1 — Dalin = 11.2 — **- inner diameter of Al** (mm)

Aall := Rep0,4 — Asc = 74.88 — **- total area of steel core** (mm²)

Aal := Rep0,7 — Aall = 0 — **- total area of alloy** (mm²)

Rsteel := | 1/Rep0,2 if Rep0,2 > 0 | 0 otherwise — Aal = 605.99 — **- total area of aluminium** (mm²)

Rsteel = 0.003 — **- resistance of steel core** (Ω/m)

Rall := | 1/Rep0,5 if Rep0,5 > 0 | 0 otherwise — Rall = 0 — **- resistance of alloy layers** Ω/m)

Ral := | 1/Rep0,8 if Rep0,8 > 0 | 0 otherwise — Ral = 0 — **- resistance of aluminium** (Ω/m)

Skin effect calculation:

- steel core:

Skin := 1. — - skin effect for steel core not assumed:

Rsteel := Skin · Rsteel — Rsteel = 0.003 — - steel core resistance, corrected by skin effect

- alloy layer:

$$\alpha 0 := \sqrt{\pi^2 \cdot \frac{f}{\rho aal \cdot 10^5}} - i \cdot \sqrt{\pi^2 \cdot \frac{f}{\rho aal \cdot 10^5}}$$ — α0 = 0.388 − 0.388i — - propagation constant

$$\alpha 0X := Re(\alpha 0) \cdot \frac{Dallou}{20} + i \cdot Im(\alpha 0) \cdot \frac{Dallou}{20}$$ — α0X = 0 — - Bessel function input parameter

$$\alpha 0x := Re(\alpha 0) \cdot \frac{Dallin}{20} + i \cdot Im(\alpha 0) \cdot \frac{Dallin}{20}$$ — α0x = 0 — "

Bes := ber(1, −|α0X|) + i · bei(1, −|α0X|) — Bes = 0 — - Bessel function values

Bex := ber(0, −|α0x|) + i · bei(0, −|α0x|) — Bex = 1 — "

Bet := ber(0, −|α0X|) + i · bei(0, −|α0X|) — Bet = 1 — "

$$ir := \frac{\frac{\alpha 0X}{2} \cdot Bex}{Bes}$$

Skip := | ir · |Bet| if |ir| · Bet > 0 | 1 otherwise

Skin := Re(Skip) — Skin = 1

Rall := Skin · Rall — Rall = 0 — - alloy layer resistance, corrected by skin effect

- aluminium layer:

$$\alpha Q := \sqrt{\pi^2 \cdot \frac{f}{\rho al \cdot 10^5}} - i \cdot \sqrt{\pi^2 \cdot \frac{f}{\rho al \cdot 10^5}} \qquad \alpha Q = 0.419 - 0.419i$$ - propagation constant:

$$\alpha QX := Re(\alpha Q) \cdot \frac{Dalou}{20} + i \cdot Im(\alpha Q) \cdot \frac{Dalou}{20} \qquad \alpha QX = 0.71 - 0.71i$$ - Bessel function input parameter

$$\alpha Qx := Re(\alpha Q) \cdot \frac{Dalin}{20} + i \cdot Im(\alpha Q) \cdot \frac{Dalin}{20} \qquad \alpha Qx = 0.235 - 0.235i$$

$Bes := ber(1, -|\alpha QX|) + i \cdot bei(1, -|\alpha QX|)$ $\quad Bes = 0.398 - 0.308i$ - Bessel function values

$Bex := ber(0, -|\alpha Qx|) + i \cdot bei(0, -|\alpha Qx|)$ $\quad Bex = 1 + 0.028i$ "

$Bet := ber(0, -|\alpha QX|) + i \cdot bei(0, -|\alpha QX|)$ $\quad Bet = 0.984 + 0.251i$ "

$$ir := \frac{\frac{\alpha QX}{2} \cdot Bex}{Bes}$$

$$Skip := \begin{cases} ir \cdot |Bet| & \text{if } |ir| > 0 \\ 1 & \text{otherwise} \end{cases} \qquad Skip = 1.008 - 0.099i$$

$Skin := Re(Skip)$ $\quad Skin = 1.008$

$Ral := Skin \cdot Ral$ $\quad Ral = 59.187 \times 10^{-6}$ - aluminium layer resistance, corrected by skin effect

$$Rcon := \begin{cases} Rcon \leftarrow 0 \\ Rcon \leftarrow \frac{1}{Rsteel} & \text{if } Rsteel > 0 \\ Rcon \leftarrow Rcon + \frac{1}{Rall} & \text{if } Rall > 0 \\ Rcon \leftarrow Rcon + \frac{1}{Ral} & \text{if } Ral > 0 \\ Rcon \leftarrow \frac{1}{Rcon} \end{cases} \qquad Rcon = 58.024 \times 10^{-6}$$ - conductor resistance (Ω/m, corrected by skin effect

DC current distribution:

$Itot := 1500$ - first assumption of total current (A)

$Itop := Itot$

$$I_i := \left(Itot \cdot \frac{Rcon}{Rdc_i}\right) \qquad \begin{pmatrix} 1.564 \\ 9.358 \end{pmatrix}$$

DC current distribution:

$\begin{pmatrix} 0.397 \\ 0.396 \end{pmatrix}$ $\quad \begin{pmatrix} 0.087 \\ 0.087 \end{pmatrix}$

3	600
4	800
5	1000
6	1200
7	1400
8	1600
9	1800
10	2000
11	2200
12	2400
13	2600

3	75
4	108
5	153
6	188
7	216
8	236
9	252
10	265
11	276
12	282
13	284

3	47
4	116
5	194
6	262
7	290
8	300
9	287
10	269
11	248
12	226
13	203

$x := 0, 10 .. 2600$

interp (vp, Hm, Mi, x)

interp (vs, Hm, Mr, x)

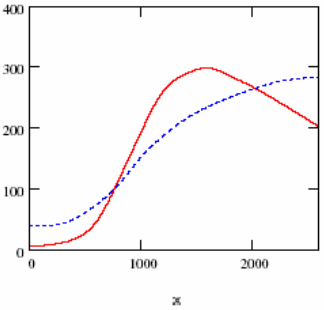

$x := H$

$\mu r := interp(vs, Hm, Mr, x) - i \cdot interp(vp, Hm, Mi, x)$

$\mu r = 180.339 - 248.536i$ - relative permeability of steel

$j := 0 .. NI - 1$

$$\mu r_j := \begin{cases} \mu r & \text{if } MatCod_j = 1 \\ 1 & \text{otherwise} \end{cases} \qquad \mu r = \begin{pmatrix} 180.339 - 248.536i \\ 180.339 - 248.536i \\ 180.339 - 248.536i \\ 1 \\ 1 \\ 1 \end{pmatrix}$$ - relative permeability per layer

Current dispacement assumtion:

$Kout := 0.79$ - for outer flux

$Kint := 1 - Kout$

$Kint = 0.21$ - for inner flux

REACTANCE MATRIX - first assumption:

$j := 1 .. NI - 1$

$i := 1 .. NI - 1$

$$X_{i,j} := i \cdot 2 \cdot \pi \cdot f \cdot \mu_0 \cdot \frac{\left[\left(\frac{\pi}{4}\right) \cdot (D_i)^2 - Asc\right] + \mu r_0 \cdot Asc}{\lambda_i \cdot \lambda_j}$$

$X_{j,i} := X_{i,j}$

$$X = \begin{pmatrix} 0\times 10^{0} & 0\times 10^{0} & 0\times 10^{0} & 0\times 10^{0} & 0\times 10^{0} & 0\times 10^{0} \\ 0\times 10^{0} & 1.91\times 10^{-4}+1.38i\times 10^{-4} & 2.02\times 10^{-4}+1.47i\times 10^{-4} & 1.28\times 10^{-4}+9.45i\times 10^{-5} & 1.01\times 10^{-4}+7.6i\times 10^{-5} & 7.99\times 10^{-5}+6.16i\times 10^{-5} \\ 0\times 10^{0} & 2.02\times 10^{-4}+1.47i\times 10^{-4} & 2.13\times 10^{-4}+1.55i\times 10^{-4} & 1.36\times 10^{-4}+9.99i\times 10^{-5} & 1.07\times 10^{-4}+8.03i\times 10^{-5} & 8.45\times 10^{-5}+6.51i\times 10^{-5} \\ 0\times 10^{0} & 1.28\times 10^{-4}+9.45i\times 10^{-5} & 1.36\times 10^{-4}+9.99i\times 10^{-5} & 8.63\times 10^{-5}+6.36i\times 10^{-5} & 6.81\times 10^{-5}+5.11i\times 10^{-5} & 5.38\times 10^{-5}+4.14i\times 10^{-5} \\ 0\times 10^{0} & 1.01\times 10^{-4}+7.6i\times 10^{-5} & 1.07\times 10^{-4}+8.03i\times 10^{-5} & 6.81\times 10^{-5}+5.11i\times 10^{-5} & 5.37\times 10^{-5}+4.03i\times 10^{-5} & 4.24\times 10^{-5}+3.27i\times 10^{-5} \\ 0\times 10^{0} & 7.99\times 10^{-5}+6.16i\times 10^{-5} & 8.45\times 10^{-5}+6.51i\times 10^{-5} & 5.38\times 10^{-5}+4.14i\times 10^{-5} & 4.24\times 10^{-5}+3.27i\times 10^{-5} & 3.35\times 10^{-5}+2.58i\times 10^{-5} \end{pmatrix}$$

CIRCULAR FLUX REACTANCE :

Flux :=
for $k \in 0 .. NI-2$
  for $l \in k+1 .. NI-1$
    $Lok_{k,l} \leftarrow i\cdot(f\cdot\mu_0)\cdot\left(Kint\cdot\ln\left(\frac{D_l - dw_l}{D_l}\right)\right) + i\cdot(f\cdot\mu_0)\cdot\left(Kout\cdot\ln\left(\frac{D_l}{D_l - dw_l}\right)\right)$
for $k \in 1 .. NI-1$
  for $l \in 1 .. NI-1$
    $Lok_{k,l} \leftarrow i\cdot(f\cdot\mu_0)\cdot Kout\cdot\ln\left(\frac{D_k}{D_k - dw_k}\right)$ if $k = l$
for $k \in 0 .. NI-2$
  for $l \in k .. NI-2$
    $Lop_{k,l} \leftarrow i\cdot(f\cdot\mu_0)\cdot\left(\ln\left(\frac{D_{NI-1} - dw_{NI-1}}{D_l}\right) + \ln\left(\frac{D_{NI-1}}{D_{l+1} - dw_{l+1}}\right)\right)$
  $Lop_{NI-1,NI-1} \leftarrow 0$
for $l \in 0 .. NI-1$
  for $k \in 0 .. NI-1$
    $Lok_{k,l} \leftarrow Lok_{l,k}$
    $Lop_{k,l} \leftarrow Lop_{l,k}$
$Flux \leftarrow Lok + Lop$

$$Flux = \begin{pmatrix} 2.904i\times 10^{-4} & 1.926i\times 10^{-4} & 1.215i\times 10^{-4} & 6.351i\times 10^{-5} & 2.151i\times 10^{-5} & 4.311i\times 10^{-6} \\ 1.926i\times 10^{-4} & 1.979i\times 10^{-4} & 1.215i\times 10^{-4} & 6.351i\times 10^{-5} & 2.151i\times 10^{-5} & 4.311i\times 10^{-6} \\ 1.215i\times 10^{-4} & 1.215i\times 10^{-4} & 1.245i\times 10^{-4} & 6.351i\times 10^{-5} & 2.151i\times 10^{-5} & 4.311i\times 10^{-6} \\ 6.351i\times 10^{-5} & 6.351i\times 10^{-5} & 6.351i\times 10^{-5} & 6.648i\times 10^{-5} & 2.151i\times 10^{-5} & 4.311i\times 10^{-6} \\ 2.151i\times 10^{-5} & 2.151i\times 10^{-5} & 2.151i\times 10^{-5} & 2.151i\times 10^{-5} & 2.356i\times 10^{-5} & 4.311i\times 10^{-6} \\ 4.311i\times 10^{-6} & 4.311i\times 10^{-6} & 4.311i\times 10^{-6} & 4.311i\times 10^{-6} & 4.311i\times 10^{-6} & 5.872i\times 10^{-6} \end{pmatrix}$$

IMPEDANCE MATRIX, first assumption:

```
Z := | for k ∈ 0 .. Nl − 1
     |   for l ∈ 0 .. Nl − 1
     |     Res_{k,l} ← Rdc_k
     |     Res_{k,l} ← 0  if k ≠ l
     | for k ∈ 0 .. Nl − 1
     |   for l ∈ 0 .. Nl − 1
     |     Z_{k,l} ← Res_{k,l} + SGN_k · SGN_l · X_{k,l} + Flux_{k,l}
     |     Z_{l,k} ← Res_{l,k} + SGN_l · SGN_k · X_{l,k} + Flux_{l,k}
     | Z ← Z

Zp := Z
```

$$Z = \begin{pmatrix} 5.6\times 10^{-2} + 2.9i\times 10^{-4} & 1.9i\times 10^{-4} & 1.2i\times 10^{-4} & 6.4i\times 10^{-5} & 2.2i\times 10^{-5} & 4.3i\times 10^{-6} \\ 1.9i\times 10^{-4} & 9.5\times 10^{-3} + 3.4i\times 10^{-4} & -2\times 10^{-4} - 2.5i\times 10^{-5} & 1.3\times 10^{-4} + 1.6i\times 10^{-4} & -1\times 10^{-4} - 5.4i\times 10^{-5} & 8\times 10^{-5} + 6.6i\times 10^{-5} \\ 1.2i\times 10^{-4} & -2\times 10^{-4} - 2.5i\times 10^{-5} & 4.9\times 10^{-3} + 2.8i\times 10^{-4} & -1.4\times 10^{-4} - 3.6i\times 10^{-5} & 1.1\times 10^{-4} + i\times 10^{-4} & -8.4\times 10^{-5} - 6.1i\times 10^{-5} \\ 6.4i\times 10^{-5} & 1.3\times 10^{-4} + 1.6i\times 10^{-4} & -1.4\times 10^{-4} - 3.6i\times 10^{-5} & 3.5\times 10^{-4} + 1.3i\times 10^{-4} & -6.8\times 10^{-5} - 3i\times 10^{-5} & 5.4\times 10^{-5} + 4.6i\times 10^{-5} \\ 2.2i\times 10^{-5} & -1\times 10^{-4} - 5.4i\times 10^{-5} & 1.1\times 10^{-4} + i\times 10^{-4} & -6.8\times 10^{-5} - 3i\times 10^{-5} & 2.3\times 10^{-4} + 6.4i\times 10^{-5} & -4.2\times 10^{-5} - 2.8i\times 10^{-5} \\ 4.3i\times 10^{-6} & 8\times 10^{-5} + 6.6i\times 10^{-5} & -8.4\times 10^{-5} - 6.1i\times 10^{-5} & 5.4\times 10^{-5} + 4.6i\times 10^{-5} & -4.2\times 10^{-5} - 2.8i\times 10^{-5} & 1.7\times 10^{-4} + 3.2i\times 10^{-5} \end{pmatrix}$$

AC current distribution calculation, using matrix representation:

Result :=

$Zpp \leftarrow Zp$

$i \leftarrow 0$

$Ip \leftarrow I$

$\lambda p \leftarrow \lambda$

$I_i \leftarrow lsolve\ (Zpp, \Delta V)$

$H_i \leftarrow H$

while $i < 25$

$I_i \leftarrow Ip$

for $k \in 1 .. Nl - 1$

$Hh_k \leftarrow 1000 \cdot \left(SGN_k \cdot \frac{Ip_k}{\lambda p_k} \right)$

$H \leftarrow \left| \sum Hh \right|$

$x \leftarrow H$

$\mu r_i \leftarrow interp\ (vs, Hm, Mr, x) \quad - i \cdot \ (interp\ (vp, Hm, Mi, x)\ )$

for $k \in 1 .. Nl - 1$

for $l \in 1 .. Nl - 1$

$X_{k,l} \leftarrow i \cdot \left[2 \cdot \pi \cdot f \cdot \mu_0 \cdot \frac{\left[\left(\frac{\pi}{4} \right) \cdot (D_k)^2 - Asc \right] + \mu r_i \cdot Asc}{\lambda_k \cdot \lambda_l} \right]$

$X_{l,k} \leftarrow X_{k,l}$

for $k \in 0 .. Nl - 1$

for $l \in 0 .. Nl - 1$

$Res_{k,l} \leftarrow R20_k \cdot \left[1 + \alpha_k \cdot (t_k - 20)\right]$

$Res_{k,l} \leftarrow 0 \quad \text{if} \quad k \neq l$

for $k \in 0 .. Nl - 1$

for $l \in 0 .. Nl - 1$

$Z_{k,l} \leftarrow Res_{k,l} + SGN_k \cdot SGN_l \cdot X_{k,l} + Flux_{k,l}$

$Z_{l,k} \leftarrow Res_{l,k} + SGN_k \cdot SGN_l \cdot X_{l,k} + Flux_{l,k}$

$I_i \leftarrow lsolve\ (Z, \Delta V)$

$Ip \leftarrow I_i$

$ki \leftarrow \frac{Itop}{\left|\sum Ip\right|}$

$\Delta V \leftarrow \Delta V \cdot ki$

$\mu r \leftarrow \mu r_i$

$i \leftarrow i + 1$

$\Delta V \leftarrow \Delta V$

$(Ip \quad Z \quad \mu r \quad \Delta V \quad H)$

Current distribution in each layer:

$$Result_{0,0} = \begin{pmatrix} 1.42 - 0.629i \\ 6.601 - 4.4i \\ 20.914 - 5.973i \\ 257.846 - 142.379i \\ 544.111 - 103.877i \\ 629.056 - 73.77i \end{pmatrix}$$

$j := 0 .. Nl - 1$

$$j_j := \frac{\left|(Result_{0,0})_j\right|}{A_j}$$

$$i = \begin{pmatrix} 0.394 \\ 0.335 \\ 0.46 \\ 2.187 \\ 2.742 \\ 2.352 \end{pmatrix}$$

- current density (A/mm^2) per layer

RESISTANCES:

$$Zep := \frac{\sum Result_{0,3}}{\frac{Nl}{\sum Result_{0,0}}}$$

$Zep = 6.03 \times 10^{-5} + 1.367i \times 10^{-5}$ - conductor impedance (Ω/m)

$Rac := Re\ (Zep)$

$Rac = 6.03 \times 10^{-5}$ - AC resistance (Ω/m)

$kred := \frac{|Zep|}{Rcon}$

$kred = 1.066$ - AC/DC ratio (current redistrbution factor)

$tcor := tc$

$tcor = 80$ - core temperature (deg.C, assumption)

MAGNETIC FIELD:

$Bm := \mu_0 \cdot \left|Result_{0,2}\right| \cdot \sqrt{2} \cdot Result_{0,4}$

$Bm = 0.223$ (T/m)

$$\Delta R := \frac{Pmagnetic}{\left[Itot \cdot \left(1 - \frac{Rcon}{Rsteel}\right)\right]^2}$$

$\Delta R = 1.725 \times 10^{-7}$ (Ω/m)

$$km := \frac{\Delta R}{Rcon}$$

$km = 0.003$ - AC/DC ratio increment due to magnetic losses

Magnetic losses component:

$$Pmagnetic := 160 \cdot f \cdot \gamma st \cdot \sqrt{dw_0} \cdot Asc \cdot Bm^{1.82} \cdot e^{-2.5 tcor 10^{-3}} \cdot 10^{-6}$$

$Pmagnetic = 0.373$ (W/m)

$Kacdc := kred + km$

$Kacdc = 1.069$ - **total AC/DC ratio (without skin effect)**

ANALYSIS:

- Total AC/DC ratio for Grackle (example above, **single** Al layer assumption)

Current (A)	Skin effect contribution	Current redistribution increment	Magnetic losses increment	Total AC/DC resistance ratio
0	0.000	0.000	0.000	1.000
250	0.001	0.094	0.016	1.111
500	0.001	0.288	0.077	1.366
750	0.001	0.289	0.084	1.374
1000	0.001	0.220	0.069	1.290
1250	0.001	0.095	0.046	1.142
1500	0.001	0.022	0.030	1.053

$I :=$

	0
0	0
1	250
2	500
3	750
4	1000
5	1250
6	1500

$Cr :=$

	0
0	0
1	0.094
2	0.288
3	0.289
4	0.22
5	0.095
6	0.022

$MI :=$

	0
0	0
1	0.016
2	0.077
3	0.084
4	0.069
5	0.046
6	0.03

Measured values (Barrett) :

$$lk := \begin{pmatrix} 50 \\ 120 \\ 185 \\ 260 \\ 390 \\ 510 \\ 610 \\ 700 \\ 810 \\ 910 \\ 1010 \\ 1110 \\ 1220 \\ 1330 \\ 1450 \\ 1580 \end{pmatrix} \quad kr := \begin{pmatrix} 1.01 \\ 1.025 \\ 1.05 \\ 1.12 \\ 1.25 \\ 1.38 \\ 1.42 \\ 1.44 \\ 1.42 \\ 1.39 \\ 1.36 \\ 1.33 \\ 1.30 \\ 1.27 \\ 1.25 \\ 1.23 \end{pmatrix}$$

$x := 0 , 10 .. 1500$

$ys := lspline (l, Cr)$

$yp := lspline (l, Ml)$

interp (yp, l, Ml+1, x)

interp (ys, l, Cr+1, x)

interp (yp+ys, l, Ml+Cr+1.001, x)

kr

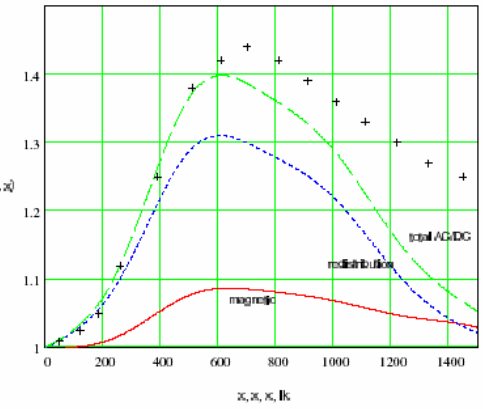

Total AC/DC ratio for Grackle (example above, **twin** Al layer assumption)

Current (A)	Skin effect contribution	Current redistribution increment	Magnetic losses increment	Total AC/DC resistance ratio
0	0.000	0.000	0.000	1.000
250	0.004	0.0005	0.0001	1.0006
500	0.004	0.004	0.0001	1.0041
750	0.004	0.0043	0.0001	1.0044
1000	0.004	0.0041	0.0001	1.0042
1250	0.004	0.004	0.0001	1.0041
1500	0.004	0.004	0.0001	1.0041

I :=

	0
0	0
1	250
2	500
3	750
4	1000
5	1250
6	1500

Cr :=

	0
0	0
1	0.0005
2	0.004
3	0.0043
4	0.0041
5	0.004
6	0.004

Ml :=

	0
0	0
1	0.0001
2	0.0001
3	0.0001
4	0.0001
5	0.0001
6	0.0001

Measured values (Barrett) :

$$lk := \begin{pmatrix} 100 \\ 130 \\ 250 \\ 380 \\ 480 \\ 710 \\ 970 \\ 1190 \end{pmatrix} \quad kr := \begin{pmatrix} 1.002 \\ 1.0058 \\ 1.005 \\ 1.0056 \\ 1.0052 \\ 1.0045 \\ 1.004 \\ 1.0053 \end{pmatrix}$$

vs := lspline (I, Ml)

vp := lspline (I, Cr)

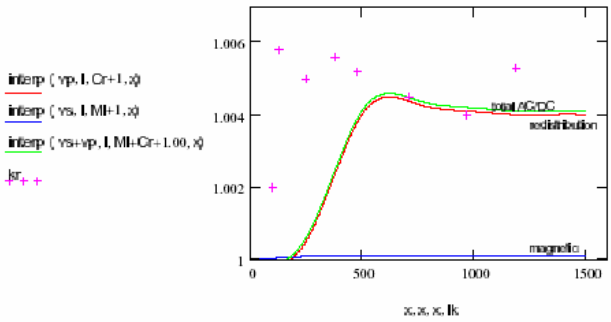

- Total AC/DC ratio for Grackle (**three** Al layer assumption)

Current (A)	Skin effect contribution	Current redistribution increment	Magnetic losses increment	Total AC/DC resistance ratio
0	0.000	0.000	0.000	1.000
250	0.008	0.040	0.001	1.049
500	0.008	0.042	0.001	1.051
750	0.008	0.047	0.001	1.056
1000	0.008	0.053	0.002	1.063
1250	0.008	0.058	0.002	1.068
1500	0.008	0.066	0.003	1.077
1750	0.008	0.073	0.004	1.085
2000	0.008	0.077	0.005	0.090
2250	0.008	0.078	0.005	0.091
2500	0.008	0.077	0.005	0.090

I :=

	0
0	0
1	250
2	500
3	750
4	1000
5	1250
6	1500
7	1750
8	2000
9	2250
10	2500

Cr :=

	0
0	0.039
1	0.04
2	0.042
3	0.047
4	0.053
5	0.058
6	0.066
7	0.073
8	0.077
9	0.078
10	0.077

Ml :=

	0
0	0.001
1	0.001
2	0.001
3	0.001
4	0.002
5	0.002
6	0.003
7	0.004
8	0.005
9	0.005
10	0.005

x := 10, 20.. 2500 vs := lspline (I, Cr) vp := lspline (I, Ml)

Measured values (Barrett, Morgan) :

B: + M: x

$$lk := \begin{pmatrix} 50 \\ 350 \\ 490 \\ 710 \\ 800 \\ 950 \\ 1210 \\ 1420 \end{pmatrix} \quad kr := \begin{pmatrix} 1.037 \\ 1.043 \\ 1.042 \\ 1.049 \\ 1.055 \\ 1.054 \\ 1.067 \\ 1.073 \end{pmatrix} \quad lkm := \begin{pmatrix} 200 \\ 400 \\ 600 \\ 800 \\ 1000 \\ 1200 \\ 1400 \\ 1600 \\ 1800 \end{pmatrix} \quad km := \begin{pmatrix} 1.033 \\ 1.038 \\ 1.042 \\ 1.054 \\ 1.065 \\ 1.073 \\ 1.080 \\ 1.087 \\ 1.091 \end{pmatrix}$$

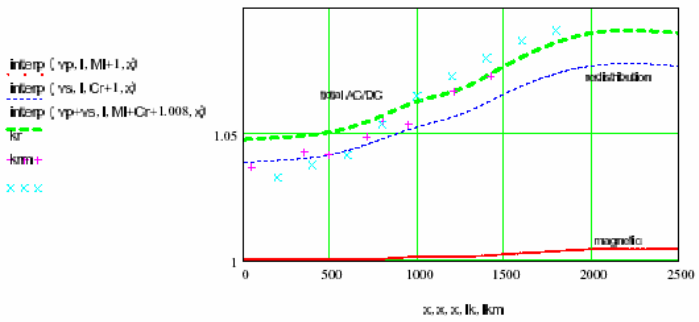

APPENDIX B

AC resistance calculation for multi-layer ACSR conductors according to a model developed by Güntner and Varga

This program was developed by Güntner and Varga based on their research and on works of Morgan, Barrett, and others. One of important features here is treating a permeability curve as an input. The geometry of the conductor can be any associated with a helically stranded conductor. It can be also be any composition of AAAC, ACSR, ACAR conductor.
The computer program was developed on the basis of theoretical model shown on Fig. B1.

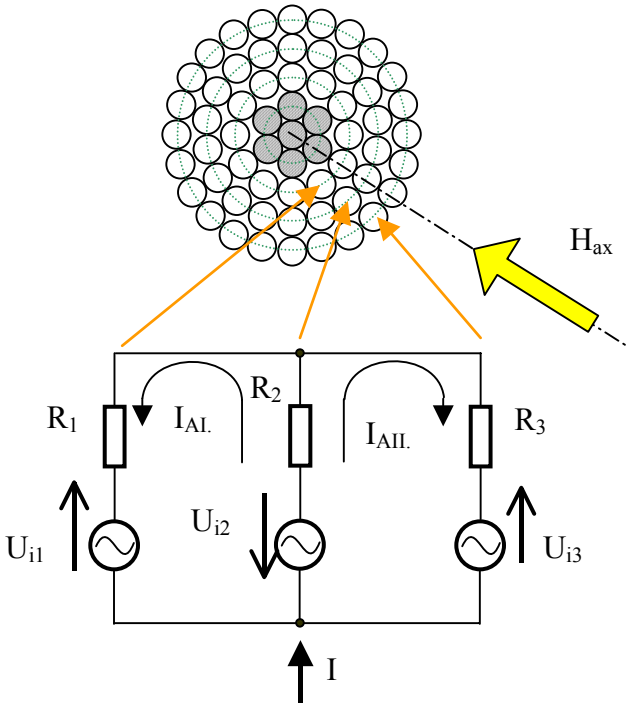

Fig. B1.
Induced voltages and currents in aluminium layers of a three-layer ACSR conductor

R_1 - R_3: Resistance of aluminium layers
U_{i1} - U_{i3}: Induced voltage in aluminium layers
I_{AI} - I_{AII}: Induced current component in aluminium layers

The axial magnetic field of steel core induces voltages in aluminium layers. The direction of the induced voltage is opposite in middle-layer, because the stranding direction is opposite in middle layer comparing to the first and the third one. The absolute values of induced voltages depend on stranding geometry of the conductor.
The induced current of middle layer caused by induced voltages increases the resultant current in the middle layer, while the induced current decreases the resultant current of first and third layer. The induced current decreases the induction of the steel core and the iron loss, while causes over-loss in aluminium layers.
According to the test results it was verified that the highest current density is not in the outside layer, caused by ”skin” effect, but in the middle-layer because of the induced current. For example, the current density of the middle layer of a three layer ACSR conductor

(500/65) is about 15-20 % higher than the average current density. The current density of layers depend on stranding geometry of conductors.
The experiments have shown that the stranding geometry has a strong effect on the current distribution and axial magnetic field, which cause the iron loss in the steel core and over-loss in the aluminum layers. The uneven current distribution decreases the magnetic field strength in the steel core. The majority of over-loss develops in the aluminum layers, but not in the steel core. On the basis of test results and theoretical studies it was shown, that the loss of ACSR conductors can be determined only by knowing the current distribution of AL-layers. Therefore substitution connection and corresponding calculation method for the stranded multi-layer conductors was developed.

The calculation model was developed by VEIKI-VNL Ltd (Fig. B2). The primary circuits substitute the aluminum layers while the secondary circuit substitutes the steel core. In the substitutions diagram "I" symbolizes the current in the conductor, which is equal to the sum of the current in each layer (I1, I2, I3). In the substitutions diagram, the secondary circuit symbolizes only the eddy-current and hysteresis losses.

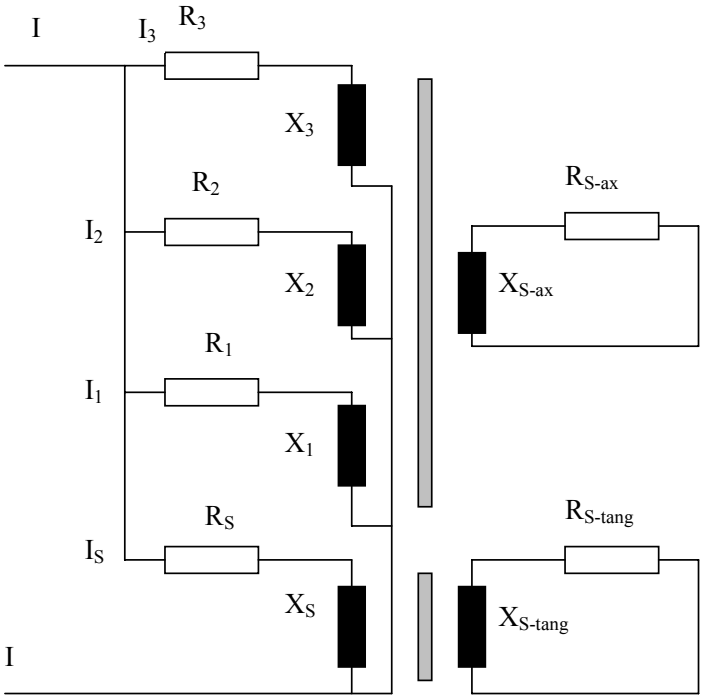

Fig. B2.
Model of the conductor completed with secondary circuits

The upper secondeary circuit symbolise the loss in the steel core caused by the axial flux that is generated by the current of the aluminum layers, and the effect of the axial flux of the steel core to the uneven current distribution of the aluminum layers.
The lower secondary circuit symbolise the inner inductance and resistance (modified by the skin effect) caused by the circular magnetic flux generated by the current in the steel core ..

Equations based on model Fig. B2.

$$I_1 \cdot (R_1 + jX_1) - I_2 \cdot jX_{1,2} + I_3 \cdot jX_{3,1} - I_{S\text{-}ax} \cdot jX_{S\text{-}ax,1} = U$$

$-I_1 \cdot jX_{1,2} + I_2 \cdot (R_2 + jX_2) - I_3 \cdot jX_{2,3} - I_{S\text{-}ax} \cdot jX_{S\text{-}ax,2} = U$

$I_1 \cdot jX_{3,1} - I_2 \cdot jX_{2,3} + I_3 \cdot (R_3 + jX_3) - I_{S\text{-}ax} \cdot jX_{S\text{-}ax,3} = U$

$-I_1 \cdot jX_{S\text{-}ax,1} + I_2 \cdot jX_{S\text{-}ax,2} - I_3 \cdot jX_{S\text{-}ax,3} + I_{S\text{-}ax} \cdot (R_{S\text{-}ax} + jX_{S\text{-}ax}) = 0$

$I_1 + I_2 + I_3 + I_S = I$

$I_S \cdot R_S + I_S \cdot jX_S + I_{S\text{-}tang} \cdot jX_{S\text{-}tang,S} = U$

$I_{S\text{-}tang} \cdot (R_{S\text{-}tang} + jX_{S\text{-}tang}) - I_S \cdot jX_{S\text{-}tang,S} = 0$

The circular magnetic flux and loss generated by the current in the steel core is difficult to calculate, because the steel core consists of separate strands. This parameter should be established by measurements.
Theoretical calculations and laboratory measurements proved that the circular magnetic flux flux caused by the current of the steel core is negligible. Therefore the model could be simplified, as shown in Fig. B3.

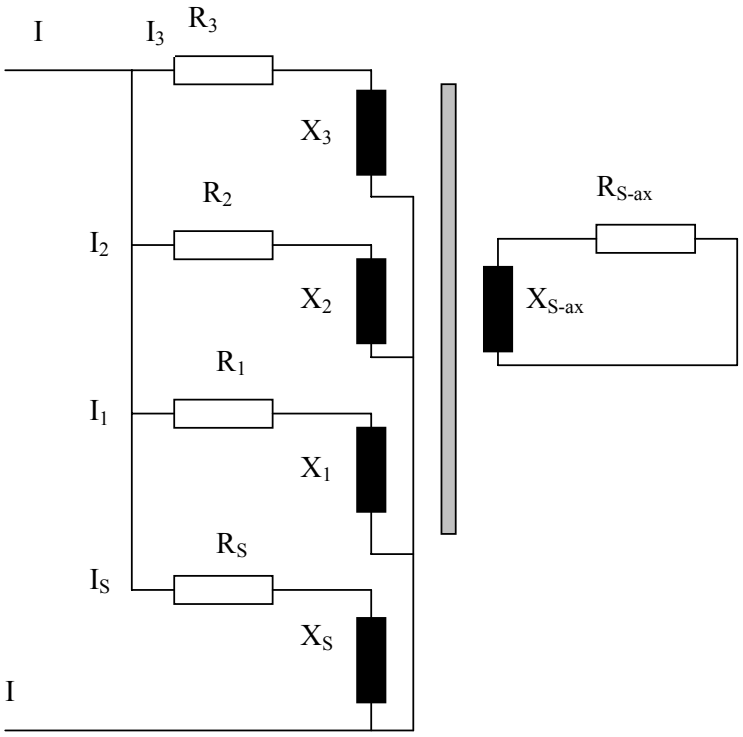

Fig. B3.
Corrected model of multi-layer conductors

$R_{s\text{-}tang}$ and $X_{s\text{-}tang}$ of the Fig.B2. can be "built into the primary circuit", and it is taken into account in the values of R_s and X_s.
R_s theoretically contains the loss caused by the circular magnetci flux in the steel wires. The circular magnetic flux in the steel wires causes skin-effect that increases the loss of steel wires. Since penetration depth is about 3mm at 50 Hz, this effect is negligible. Therefore, the DC resistance is used for R_s.

Modified equations based on model Fig. B3.

$I_1 \cdot (R_1 + jX_1) - I_2 \cdot jX_{1,2} + I_3 \cdot jX_{3,1} - I_{S\text{-}ax} \cdot jX_{S\text{-}ax,1} = U$

$-I_1 \cdot jX_{1,2} + I_2 \cdot (R_2 + jX_2) - I_3 \cdot jX_{2,3} - I_{S\text{-}ax} \cdot jX_{S\text{-}ax,2} = U$

$I_1 \cdot jX_{3,1} - I_2 \cdot jX_{2,3} + I_3 \cdot (R_3 + jX_3) - I_{S\text{-}ax} \cdot jX_{S\text{-}ax,3} = U$

$-I_1 \cdot jX_{S\text{-}ax,1} + I_2 \cdot jX_{S\text{-}ax,2} - I_3 \cdot jX_{S\text{-}ax,3} + I_{S\text{-}ax} \cdot (R_{S\text{-}ax} + jX_{S\text{-}ax}) = 0$

$I_1 + I_2 + I_3 + I_S = I$

$I_S \cdot R_S + I_S \cdot jX_S = U$

Parameters of aluminum layers:

$$R_i = \frac{l \cdot \rho_{al}}{\sin \alpha_i \cdot n_i \cdot r_i^2 \cdot \pi} \qquad \alpha_i = arctg\left[\frac{Layratio_i}{\pi \cdot \left(1 - \frac{2 \cdot r_i}{D_i}\right)}\right]$$

$$X_i = \omega \cdot \mu \cdot A_{st} \cdot \frac{N_i^2}{l} \qquad N_i = \frac{l}{D_i \cdot Layratio_i}$$

$$X_{i,j} = \omega \cdot \mu \cdot A_{st} \cdot \frac{N_i \cdot N_j}{l} \qquad N_j = \frac{l}{D_j \cdot Layratio_j}$$

Parameters of secondary circuit:

$$X_{s-ax} = \omega \cdot \mu \cdot A_{st} \cdot \frac{1}{l}$$

$$X_{i,s-ax} = \omega \cdot \mu \cdot A_{st} \cdot \frac{N_i}{l}$$

$$R_{s-ax} = tg\varphi \cdot X_{s-ax}$$

$$tg\varphi = \frac{\mu_{real}}{\mu_{im}}$$

$$X_s = \frac{\omega \cdot 10^{-7} \cdot l \cdot \mu_r}{2 \cdot n_{st}}$$

where:

R_s= DC resistance of steel core (*see note 2*)
i= index of layer (i=1 .. 3 for three layers)
l= length of conductor
n_i= number of wires in the $layer_i$
n_{st}= number of wires in the steel core
r_i= radius of wires in the $layer_i$
D_i= outer diameter of $layer_i$
N_i= number of turns of wires in $layer_i$
μ_r= relative permeability of steel
μ_{real}= real component of permeability of steel
μ_{im}= imaginary component of permeability of steel

All parameters except the relative permeability values are known from conductor data sheets. Relative permeability curves of steel core shall be determined by measurements. Values measured in VEIKI-VNL Ltd. are shown in Fig.B4.

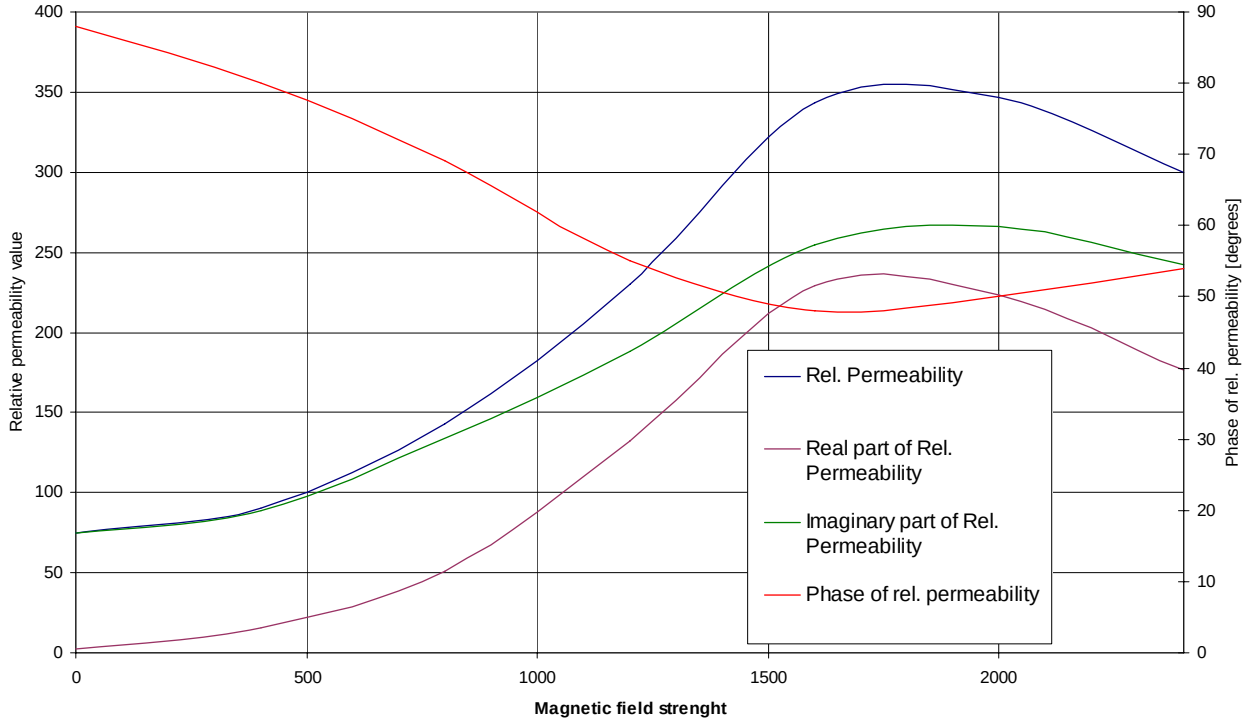

Fig. B4.
Relative permeability of steel core

These curves are approximated by the following polinoms:

Relative permeability (μ)	$y = -1^{-07}x^3 + 0{,}0003x^2 - 0{,}1084x + 78{,}19$
Phase angle of relative permeability (φ)	$y = 7^{-09}x^3 - 2E\text{-}05x^2 - 0{,}0174x + 88{,}467$
Real part of relative permeability (μ_{real})	$y = -9^{-08}x^3 + 0{,}0003x^2 - 0{,}1105x + 6{,}2951$
Imaginary part of relative permeability (μ_{imag})	$y = -6^{-08}x^3 + 0{,}0002x^2 - 0{,}0351x + 75{,}644$

Computer program was developed based on calculating method and substituion diagram (Fig. B6). Fig. B8 shows.the calculated results for ACSR 500/65 conductor.(DC, AC resistance, AC/DC resistance ratio)

Verification of the calculation method by comparison with Measurements

The results obtained from the calculation method (using a proprietory programme TENDER) were verified by laboratory measurements of ACSR conductors, with different cross sections and stranding angles. Fig.B5. shows the calculated and measured AC-resistance of ACSR

500/65 conductor with respect to loading current of the conductor. The maximum difference between calculated and measured values of Fig. B5 was less than 1,5 % [7, 8] .

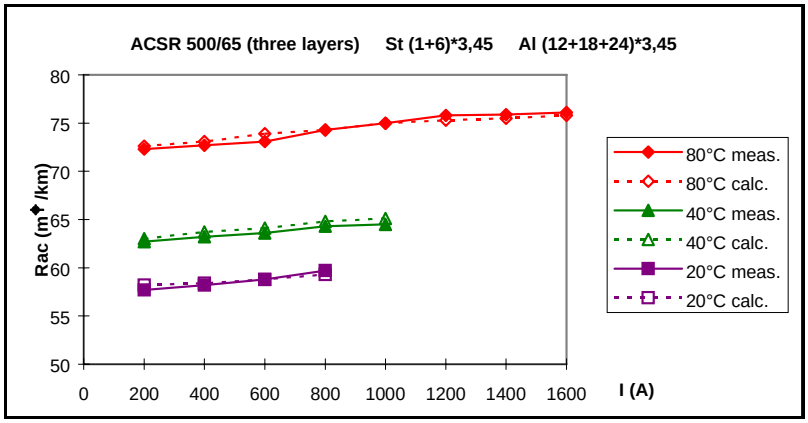

Fig. B5.
Calculated and measured AC resistance as a function of loading current (ACSR 500/65)

Fig. B6 shows AC-resistance values of four ACSR 500/65 conductors, with different stranding geometry (I.-IV.) and with the same cross section.

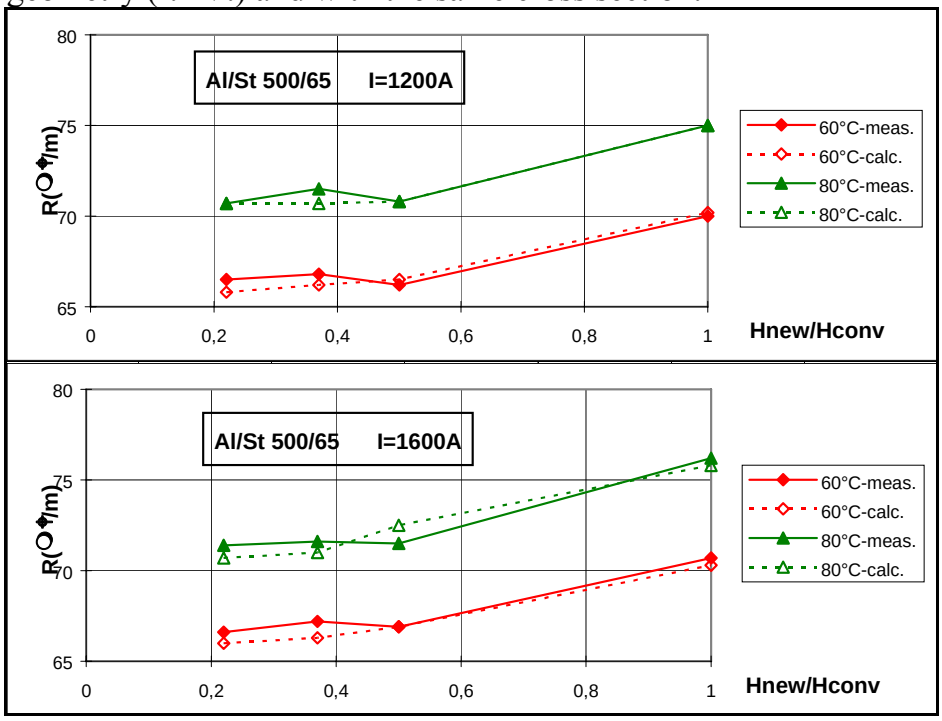

Fig. B6
Variation of AC resistance as a function of stranding geometry for four different constructions

The Fig. B6 explains the variation of AC resistance in relation to the variation of axial magnetic field in conductor. The variation of axial magnetic field depends on lay-ratios of AL wires. H_{new}/H_{conv} symbolise variation of geometry of ACSR conductor with 3 aluminium layers with the same aluminium cross section [10, 44] .

The deviation of 16 measured and computed AC resistance values is less, than 1,5% The verification of calculated method was carried out with measured values of KEMA (The Netherlands) and Furukawa(Japan) also. KEMA carried out the laboratory tests of conventional and low-loss ACSR CARDINAL conductors [5,6]. The measurements were carried out for both type of conductors within conductor temperature range of 20-120 °C and loading current range of 200-1600 A. The measured and computed values in 96 points were the same within 1-2,5%. Comparison of AC resistance ratio, measured by Furukawa and calculated by computer program are shown in Fig. B7. The maximum variation between the measured and calculated values is 2 %. The calculation method, which defines all the electrical and mechanical parameters of any kind of stranded conductors is available in form of a computer program.

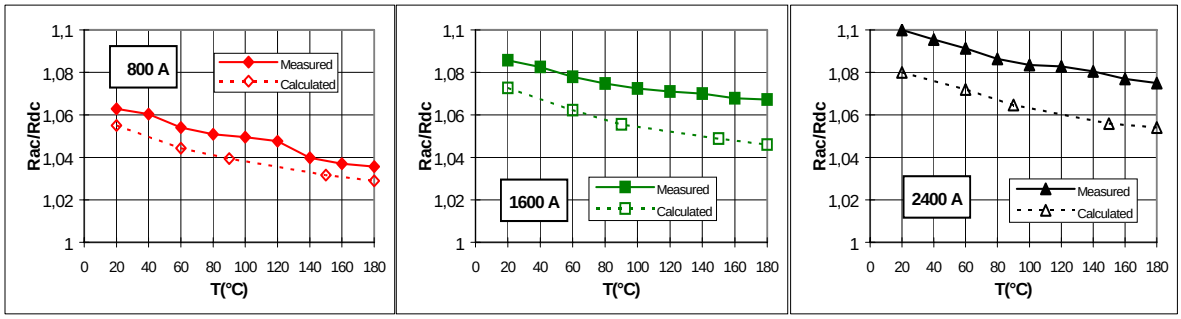

Fig. B7.

Comparison of AC-resistance ratio, measured by Furukawa and calculated by computer program developed in Research Laboratory of VEIKI

AC resistance calculation using computer program developed by Güntner and Varga

Computer program was developed using substitutional diagram and equations. The calculated results shows Fig B8.

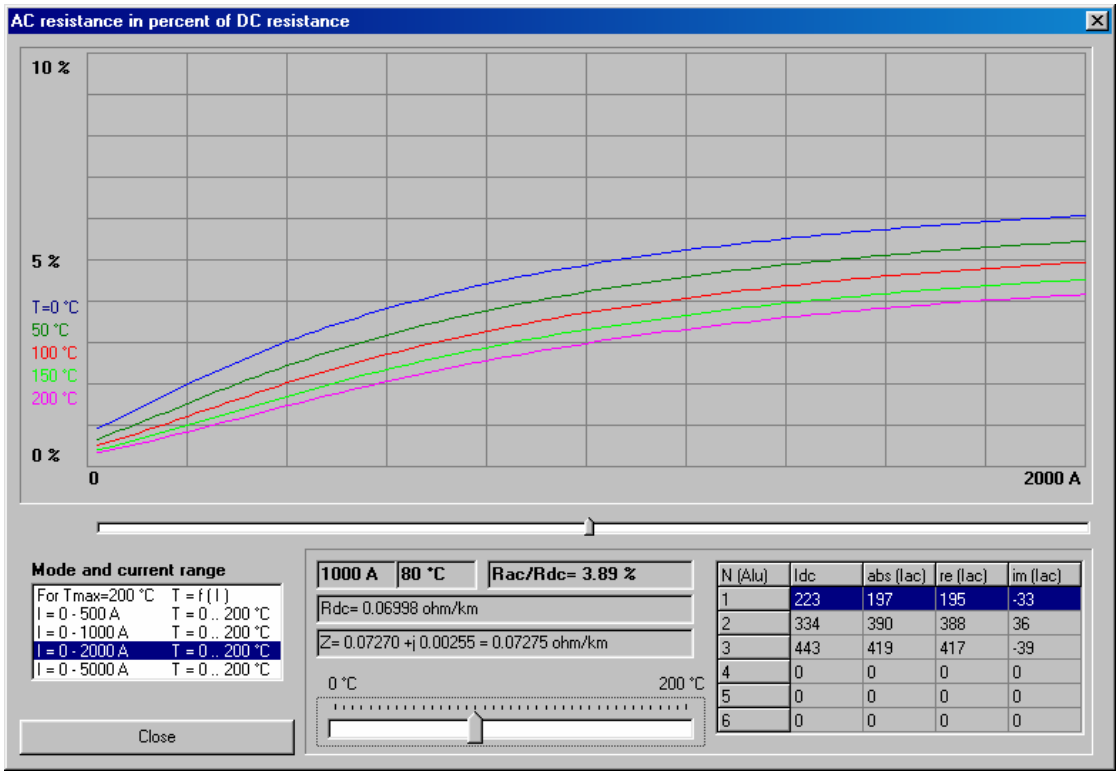

Fig. B8.
Calculated results using VEIKI-VNL software made by Güntner and Varga

Example: R_{DC} at 80°C = 0.07 Ω/km
AC resistance ratio ($K=R_{AC}/R_{DC}$) at 1000 A and 80 °C = 1.039

Data of ACSR 500/66
Steel core: 1+6 wires, 3.45 mm diameter
Alu layers: 12+18+24 wires, 3.45 mm diameter
Lay ratio of steel: 20
Lay ratio of Aluminum layer1 (outer): 12
Lay ratio of Aluminum layer2 (middle): 13
Lay ratio of Aluminum layer3 (inner): 14

Fig. B8. shows AC resistance in function of loading current.

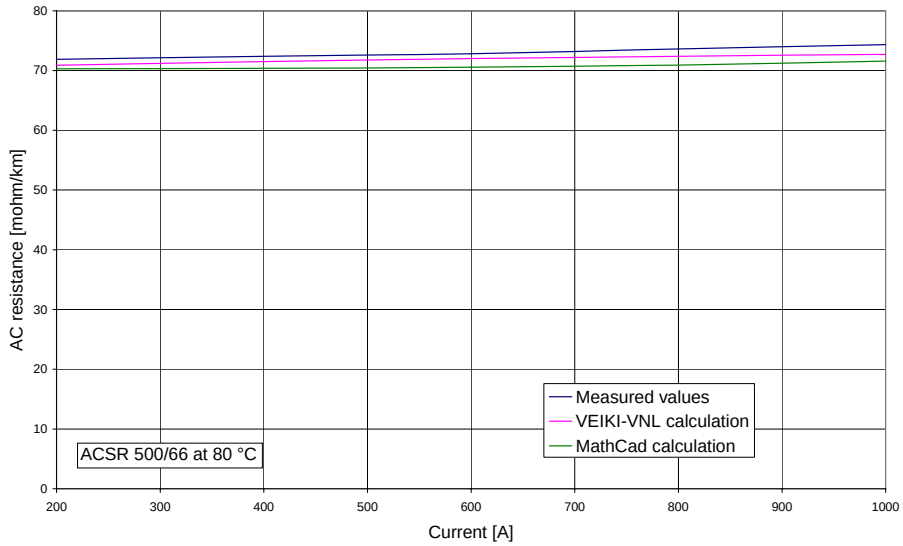

Fig. B9.
Measured and calculated results for ACSR 500/66 conductor

From the diagram it can be recognised that the two calculation programs give relatively the same results. From the diagram Fig B9. can be recognised too, that the measured AC resistance values are very closed to the calculated results with both computer programs, based on the theory of uneven current and temperature distribution of ACSR conductors.

It can be recognised too, that the calculation method, based on the theory of uneven current and temperature distribution of aluminum layers is acceptable for determination of AC resistance of ACSR conductors.

Flowchart of the computer program for AC resistance calculation as follows:

Flowchart of AC resistance calculation

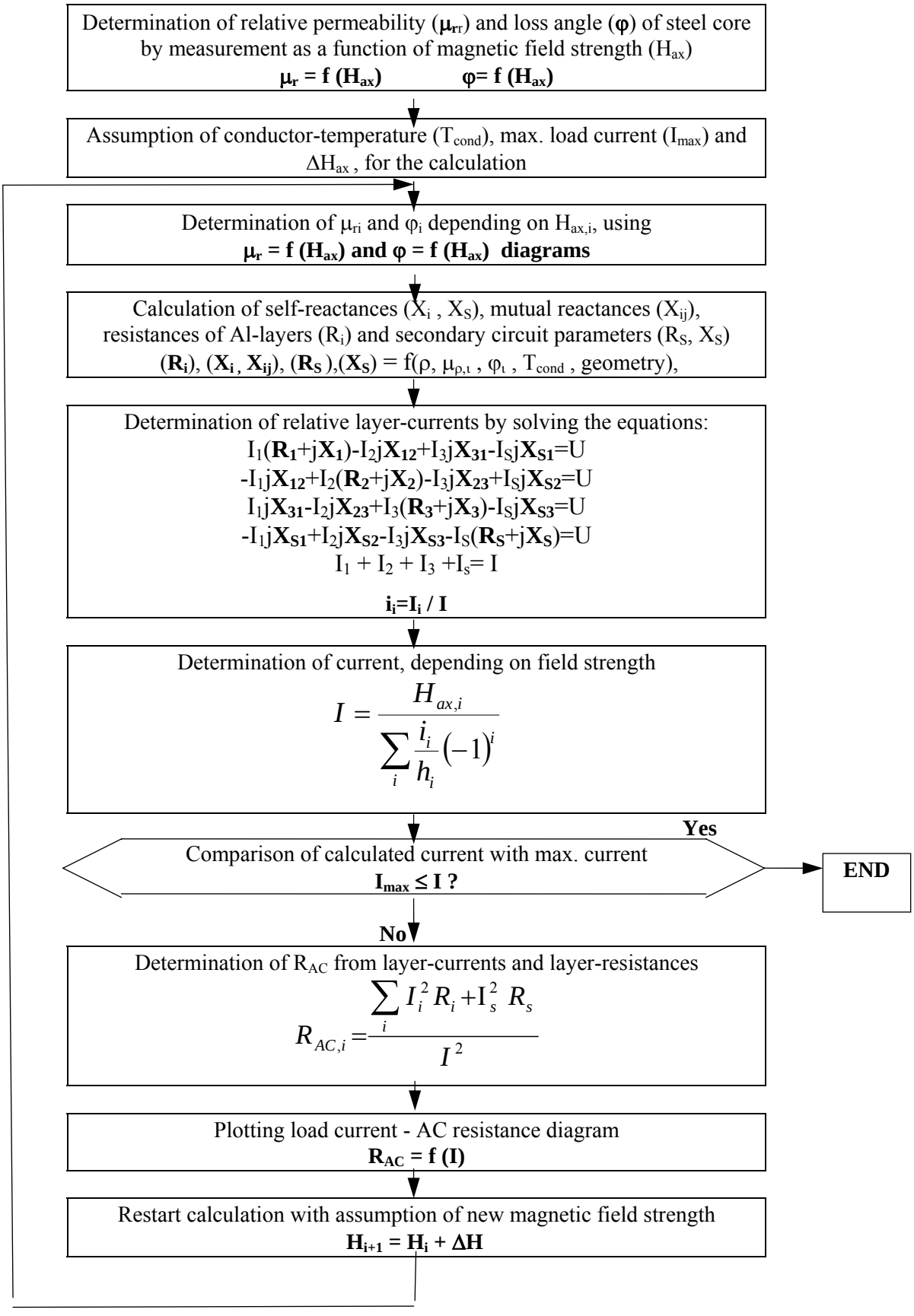

APPENDIX C MEASUREMENT OF AC RESISTANCE

1. Principle of measurement

If a conductor is powered with AC current, the impedance (Z) consists of its resistance (R_{AC}) and its inductive reactance (X_L) as shown in Fig. 1. The R_{AC} component is higher than the resistance at DC (R_{DC}).

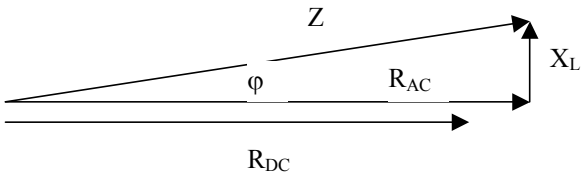

Fig 1: Impedance of the conductor

The AC resistance is basically measured the same way as the DC resistance, but the measured voltage drop will be the vector sum of the voltage on the resistive component, which is in phase with the current (U*cosφ), and the voltage on the inductive component, which is perpendicular to the current (U*sinφ).

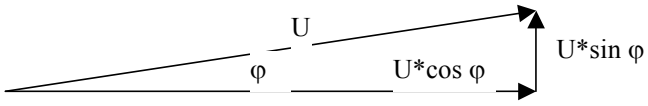

Fig 2: Components of the voltage drop on the conductor

Therefore, the AC resistance is calculated as:

$$R_{AC} = \frac{U \cdot \cos\varphi}{I}$$

where

U is the measured voltage drop on the unit length of conductor,
I is the current,
φ is the phase angle between the measured voltage and the current.

2. Test arrangement

The tested conductor is fixed in a test span and it is stressed with the required force. A conductor length of 5 m is preferred. The voltage induced by the test current in the loop formed by the tested conductor and the test leads shall be kept as low as possible. For reducing the loop area, a good practice is leading the test cables alongside the conductor to the middle, than leading to the measuring instruments by twisted cables (Fig. 3.).

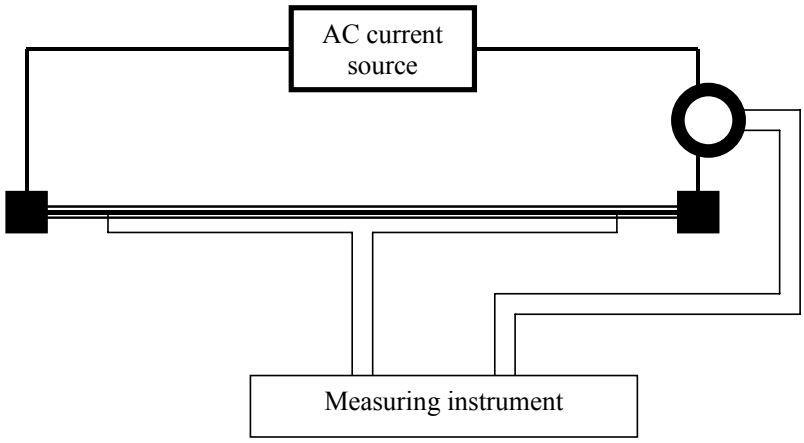

Fig 3: Test arrangement

The current is measured by a current transformer and/or shunt or current probe, depending on the input of the measuring instrument.

3. Measuring instrument

The measuring instrument can be any two-channel device, which enables accurate measurement of the voltage, the current and the phase angle between them. Selection can be made from practical aspects. Examples for suitable devices are as follows:

Wattmeter (power analyser):State of the art power analysers usually are accurate and provide direct reading of the required quantities. The voltage input shall be sensitive enough to measure the voltage drop, which is in the mV range. An additional amplifier on the voltage input may be required.

Digital storage oscilloscope or transient recorder:The sensitivity of the inputs and the accuracy are usually good, but the input is not designed for current transformers, therefore a shunt is required together with the CT, or a current probe can be used.

4. Result of the measurement

In most cases, the measured AC resistance is compared with the DC resistance and expressed as the ratio of them (R_{AC}/R_{DC} or R_{AC}-R_{DC}/R_{DC} in percents). Resistance values measured at the same conductor temperature are compared.

While the DC resistance depends on the conductor temperature only, the AC resistance depends on both the temperature and the current. Measurements at different temperature - current pairs are suggested.

Notes:

- The difference between the AC and the DC resistance is only a few percent; therefore accuracy of both the AC and the DC measurement is essential.
- The test time should be minimised to avoid undesired heating of the conductor with the test current.